Journal Pre-proofs

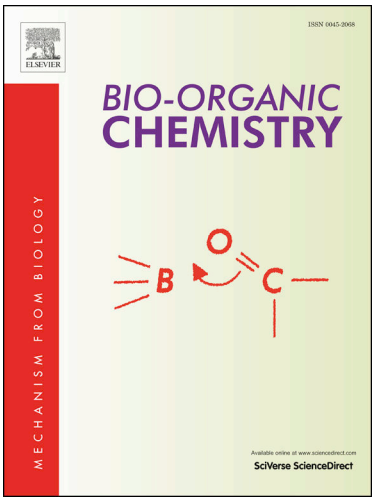


# Synthesis and biological evaluation of novel 5,6,7-trimethoxy flavonoid salicylate derivatives as potential anti-tumor agents

Renbo Liu, Xiangping Deng, Yijiao Peng, Wanshi Feng, Runde Xiong, Yang Zou, Xiaoyong Lei, Xing Zheng, Zhizhong Xie, Guotao Tang

PII: S0045-2068(19)31409-9
DOI: https://doi.org/10.1016/j.bioorg.2020.103652
Reference: YBIOO 103652

To appear in: *Bioorganic Chemistry*

Received Date: 28 August 2019
Revised Date: 1 February 2020
Accepted Date: 3 February 2020

Please cite this article as: R. Liu, X. Deng, Y. Peng, W. Feng, R. Xiong, Y. Zou, X. Lei, X. Zheng, Z. Xie, G. Tang, Synthesis and biological evaluation of novel 5,6,7-trimethoxy flavonoid salicylate derivatives as potential anti-tumor agents, *Bioorganic Chemistry* (2020), doi: https://doi.org/10.1016/j.bioorg.2020.103652

# Synthesis and biological evaluation of novel 5,6,7-trimethoxy flavonoid salicylate derivatives as potential anti-tumor agents

Renbo Liu,‡[a,b] Xiangping Deng,‡[a,b] Yijiao Peng,[a] Wanshi Feng,[a] Runde Xiong,[a] Yang Zou,[a] Xiaoyong Lei,[a] Xing Zheng,[a] Zhizhong Xie[a] and Guotao Tang*[a,b]

[a] Institute of Pharmacy and Pharmacology, Hunan Province Cooperative Innovation Center for Molecular Target New Drug Study, University of South China, Hengyang City, P.R. China.

[b]Hunan Provincial Key Laboratory of tumor microenvironment responsive drug research, Hengyang City, Hunan Province, P.R. China.

*Corresponding Author: Dr. Guotao Tang, Ph.D.

Corresponding author at：

Guotao Tang, Institute of Pharmacy and Pharmacology, University of South China, Hengyang, Hunan, 421001, People's Republic of China.

E-mail address: tgtzq@163.com (Guotao Tang)

‡ These authors contributed equally to this work.

## A B S T R A C T

5,6,7-Trimethoxy flavonoid salicylate derivatives were designed by the joining of three important pharmacophores (TMP, flavonoid, and SA) according to the combination principle. A series of novel trimethoxy flavonoid salicylate derivatives were synthesized and their *in vitro* anti-tumor activities were evaluated. Among these derivatives, compound **7f** exhibited excellent antiproliferative activity against HGC-27 cells and MGC-803 cells with $IC_{50}$ values of 10.26 ± 6.94 μM and 17.17 ± 3.03 μM, respectively. Subsequently, the effects on cell colony formation (clonogenic survival assay), cell migration (wound healing assay), cell cycle distribution (PI staining assay), cell apoptosis (Hoechst 33258 staining assay and annexin V-FITC/PI dual staining assay), lactate level (lactate measurement), microtubules disarrangement (immunofluorescence staining analysis) and docking posture (molecular docking simulation) were determined. Further western blot analysis confirmed that compound **7f** could effectively down-regulated the expression of glycolysis-related proteins HIF-1α, PFKM and PKM2 and tumor angiogenesis-related proteins VEGF. Overall, these studies suggested that compound **7f**, as the representative compound of those, maybe a promising candidate for the treatment of gastric cancer and deserving the further studies.


**Keywords**: Flavonoid; Anti-tumor; Microtubules; HIF-1α; Glycolysis



## 1. Introduction

Tumor is a kind of tissue with uncontrolled and abnormal cell proliferation, and its differentiation rate is higher than normal cells [1]. Nowadays, Cancer incidence and mortality are sharply growing in the world [2]. Hence, the development of various drugs for cancer treatment is particularly important. However, the traditional chemotherapy drugs are faced many obstacles including cytotoxicity, drug resistance and lack of sensitivity, etc [3,4]. Currently, a growing number of studies have shown that the pharmacophore combination strategy is conducive to overcome these shortcomings. A single drug molecule designed by the pharmacophore combination can act on dual/multi molecular targets which represent an efficient, logical and alternative approach to drug combinations [5]. For instance, cabometyx (cabozantinib) which has been approved by US Food and drug administration (FDA), as a small molecule dual-targeting inhibitor of the tyrosine kinases c-Met and vascular endothelial growth factor receptor 2 (VEGFR2), has been shown to reduce tumor growth, metastasis and angiogenesis [6,7].

During the last few decades, there has been an increasing interest in the approach of chemical modification of natural products aimed to improve their original biological activities. Flavonoids (Fig. 1A) as one of the vital classes of bioactive chemicals widely distribute in vegetables, fruits and medicinal plants [8,9]. Semi-synthetic and synthetic flavonoids have been reported to exhibit many therapeutic activities such as antioxidant [10], antiallergic [11], antibacterial [12], anti-inflammatory [13], antidiabetic [14], anxiolytic [15], and anticancer effects [16]. Some of the flavonoids from natural origin like silymarin, gingko flavone glycosides and naringenin, can be found in the commercial market. Simultaneously, some natural flavonoids for the auxiliary treatment of cancer or coronary heart diseases, including oroxylin A, wogonin and vitexin, are undergoing phase I/II clinical trials in China [17-19]. According to our previous research, flavonoid derivatives had performed an anti-tumor effect possibly associated with glycolysis-related proteins [20].

Furthermore, microtubule is the cage of tubulin dimers, involves in the dynamics of chromosomes specifically, mitotic spindle formation during cell division and serving as an important target for anticancer therapy [21]. Microtubule-targeting agents (MTAs) disrupt microtubule dynamic and arrest cancer cells in G2/M phase, and eventually induce apoptosis of cancer cells, which have achieved significant success in the treatment of cancer [22,23]. Some MTAs, as effective tubulin inhibitors, have entered clinical trials, such as colchicine analogs

ZD6126 [24] and CA4P [25]. MTAs have been substantiated to cause indirect tumor cell death owing to going short for oxygen and nutrients by disrupting the tumor vessels and effectively shutting off blood flow [26,27]. Another, drug resistance caused by the overexpression of the β-III tubulin isoform can be also effectively circumvented by the colchicine binding site inhibitors (CBSIs) [28]. CBSIs binds at the interface of α-subunit and b-subunit of tubulin therefore result in microtubule depolymerization. It has been demonstrated that trimethoxyphenyl (TMP) (Fig. 1B) as a common moiety for many CBSIs plays a crucial role in maintaining suitable molecular conformations for the optimal interactions with tubulin to emerge the highest-level anti-tumor efficacy [29].

Salicylic acid (SA) (Fig. 1C) is a mono-hydroxybenzoic acid that serves as a precursor of aspirin (ASA). ASA is a classic wonder drug and is widely used for the treatment of inflammation, fever and pain over a century [30]. Besides, it's reported that ASA and its metabolite SA could selectively induce apoptosis and alter tumor glucose utilization in several colorectal carcinoma cell lines [31-33]. Therefore, ASA or SA could be an outstanding anti-tumor active moiety for the development of new anticancer agents.

Given these, three important pharmacophores, including flavonoid, TMP and SA, are introduced into the design of a novel series of anti-tumor molecules according to the pharmacophore combination principle. Specifically, the trimethoxyphenyl group is introduced into the A-ring of the flavonoid and then SA and its derivatives are linked to the 4'-OH of the flavonoids with three lengths of chain alkanes (Fig. 1). The molecules are expected to inhibit the assembly of tubulin, disrupt the intracellular cytoskeleton network, and reduce the glycolytic capacity of tumor cells. Herein, the *in vitro* antitumor activity of these compounds and their effects on tubulin and glycolysis-related proteins are evaluated.

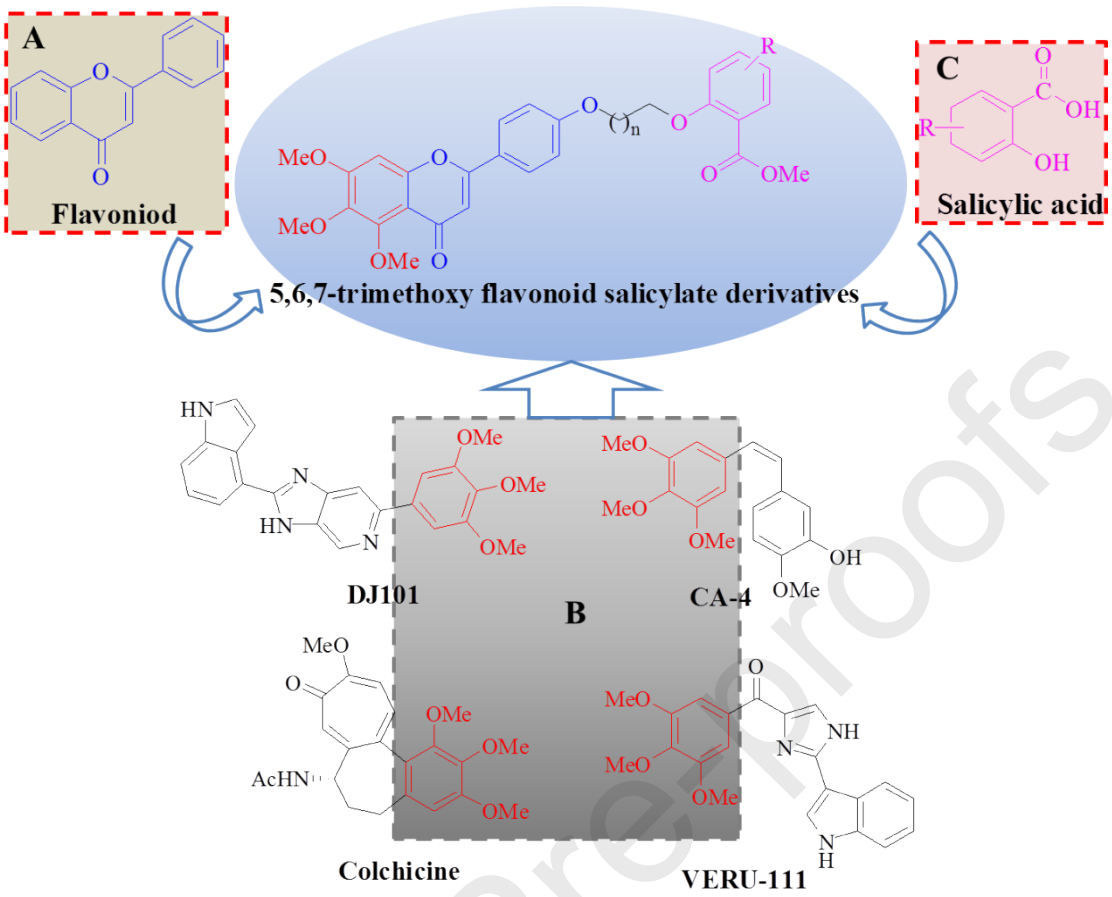


Fig. 1. The design of 5, 6, 7-trimethoxy flavonoid salicylate derivatives through the pharmacophore combination principle.

## 2. Results and discussion

### *2.1. Chemistry*

In this study, to discover new chemical entity and improve the drug-like properties, 24 flavonoid salicylate derivatives were designed and synthesized according to the general pathway shown in Scheme 1. The key intermediate 2-(4-Hydroxy-phenyl)-5,6,7-trimethoxy-chromen-4-one (**3**) was obtained via a two-step synthesis procedure, starting with 3,4,5-trimethoxy-phenol (**1**), chloroacetyl chloride and p-hydroxybenzaldehyde. First, the commercially available material **1** was used to offer 6-hydroxy-2,3,4-trimethoxy-benzoyl chloride (**2**) by the Friedel-crafts acylation under reflux conditions, with aluminum trichloride as a catalyst in dichloromethane. Then base-catalyzed aldol condensation of **2** with p-hydroxybenzaldehyde generated the chalcone, which was cyclized in the solvent of 10% hydrochloric acid and ethanol at room temperature (RT) to afford compound **3** in high yield with recrystallization from 95% ethanol. The compound **3** was treated with corresponding brominated alkanes (1,2-dibromoethane, 1,3-dibromopropane, 1,4-dibromobutane), in the presence

of potassium carbonate in a polar aprotic solvent acetone, to facilitate the formation of the alkylation product of the 4′-hydroxy group **4a-4c** in good yields. Additionally, the intermediates **6a–6h** with various types substitutions could be rashly prepared by reacting **5a–5h** with $SOCl_2$ in EtOH under reflux conditions. Eventually, etherification of the intermediates **4a–4c** and **6a–6h** to obtain the final desired compounds **7a–7x** under reflux conditions, in the presence of potassium carbonate in polar aprotic solvent acetone. All of the synthetic compounds gave adequate analytical and spectroscopic data, which agreed well with their proposed structures.

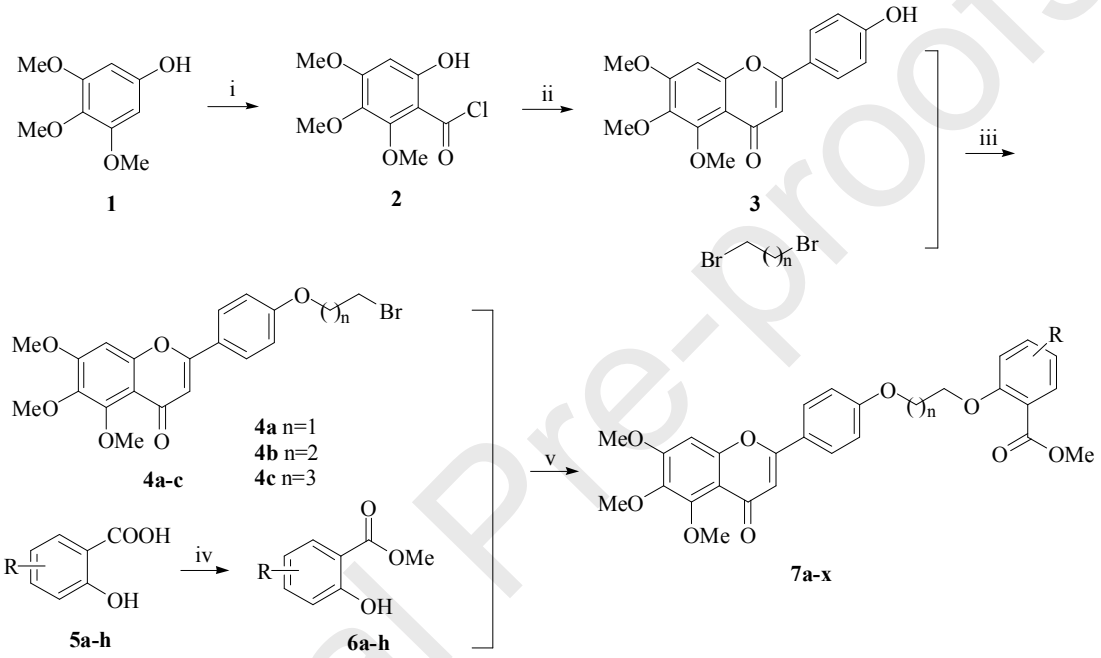


**Scheme 1.** General synthesis of 5,6,7-trimethoxy flavonoid salicylate derivatives **7a-x.** Reagents and conditions: (i) $C_2H_2Cl_2O$, $AlCl_3$, DCM, 40 °C, Reflux, 1.5 h; (ii) (a) p-hydroxybenzaldehyde, 10% NaOH, 95% Ethanol, RT, 24 h; (b) 10% HCl 1 h; (iii) $K_2CO_3$, KI Acetone, 60 °C, Reflux, 9 h; (iv) (a) $CH_3OH$,$SOCl_2$, 0 °C, 10 min; (b) 65 °C, 48 h; (v) $K_2CO_3$, KI, Acetone, Reflux, 24 h.

## *2.2. Cell proliferation*

The anti-proliferative activity *in vitro* of the novel synthesized compounds **7a–7x** was assayed against a panel of human tumor cells, MGC-803 (gastric cancer cells), HCT-116 (colon cancer cells), HGC-27 (undifferentiated gastric cancer cells), SGC-7901 (gastric carcinoma cells) and BEL-7402 (hepatoma cells), by applying 3-(4,5-dimethylthiazol-2-yl)-2,5-diphenyl tetrazolium bromide (MTT) assay. The cytotoxicity results were summarized in Table 1, which were expressed in terms of $IC_{50}$ values (the minimum concentration in μM that causes 50% of cell death concerning the control culture), where effective anti-cancer agent 5-fluorouracil (**5-FU**) was used as the positive control.

Target compounds **7a-7x** almost did not affect on SGC-7901 cells and BEL-7402 cells. Few 5,6,7-trimethoxy flavonoid salicylate derivatives displayed a little cytotoxicity against HCT-116 cell line. Additionally, some of these compounds showed passable to favorable cytotoxic activities against MGC-803 cell lines. The cytotoxicity of the synthesized novel flavonoid salicylate derivatives compounds **7a-7x** against HGC-27 cells was the best out of the five cancer cell lines. We desired to confirm whether those compounds were toxic to exhibited selective antiproliferative activities between normal cells and cancer cells, all target compounds were screened against GES-1 cells (human gastric epithelial cell line). As a whole, the benzene ring monosubstituted derivatives of SA in target compounds were more active than polysubstituted derivatives. After comparison of the biological activity data, it was observed that compounds with substitutions on the R5-position of SA showed more remarkable inhibitory activity than the R4-positioned ones, when the SA had only one position substituted on the benzene ring. Moreover, it was worth noting that the linkage of 2 carbons was presented stronger anti-proliferative activity than 3 carbons or 4 carbons against HGC-27 cells when R4-position of SA was bromine. In addition, In general, compound **7f** displayed the most potent inhibitory activity, with $IC_{50}$ of 17.17 ± 3.03 μM and 10.26 ± 6.94 μM on MGC-803 cells and HGC-27 cells, respectively, which was better than that of **5-FU** ($IC_{50}$ = 45.51 ± 13.3 μM and 17.11 ± 2.64 μM, respectively). The $IC_{50}$ of the compound **7f** on GES-1 cells was almost 2-4 times that of gastric cancer cells, indicating that the compound **7f** had certain selectivity for normal cells and cancer cells. Accordingly, compound **7f** should undergo further mechanism investigation to seek for a potentially more safe and effective chemotherapy agent.

**Table 1**

Anti-proliferative activity results of compounds **7a-7x**

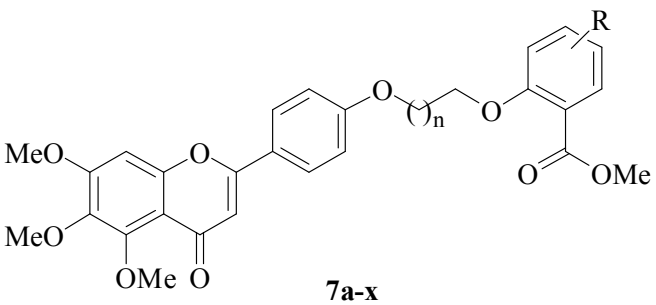


**7a-x**

| compound | n | R | $IC_{50}$ (μM) | | | | | |
|---|---|---|---|---|---|---|---|---|
| | | | SGC-7901 | MGC-803 | HGC-27 | HCT-116 | BEL-7402 | GES-1 |

| | | | | | | | | |
|---|---|---|---|---|---|---|---|---|
| **7a** | 3 | 5-$CH_3$ | N.D | > 100 | 8.74 ± 1.46 | 50.9± 7.56 | N.D | 49.16 ± 6.37 |
| **7b** | 3 | 5-Cl | N.D | > 100 | > 100 | > 100 | N.D | > 100 |
| **7c** | 3 | 5-Br | N.D | > 100 | > 100 | > 100 | N.D | N.D |
| **7d** | 2 | 5-$CH_3$ | N.D | N.D | > 100 | > 100 | N.D | N.D |
| **7e** | 2 | 5-Cl | N.D | 25.08 ± 5.07 | 14.52 ± 9.73 | > 100 | N.D | 9.88 ± 1.66 |
| **7f** | 2 | 5-Br | N.D | 17.17 ± 3.03 | 10.26 ± 6.94 | N.D | N.D | 39.01± 3.72 |
| **7g** | 1 | 5-$CH_3$ | N.D | > 100 | 66.08 ± 6.79 | > 100 | N.D | > 100 |
| **7h** | 1 | 5-Cl | N.D | > 100 | 17.32 ± 8.04 | N.D | N.D | 46.02± 5.28 |
| **7i** | 1 | 5-Br | N.D | 22.99 ± 10.4 | 9.97 ± 4.25 | N.D | N.D | 24.48± 3.64 |
| **7j** | 3 | 4-$CH_3$ | N.D | N.D | > 100 | > 100 | N.D | N.D |
| **7k** | 3 | 4-Cl | N.D | N.D | > 100 | N.D | N.D | N.D |
| **7l** | 3 | 4-Br | N.D | > 100 | > 100 | > 100 | N.D | > 100 |
| **7m** | 2 | 4-$CH_3$ | N.D | N.D | > 100 | > 100 | N.D | N.D |
| **7n** | 2 | 4-Cl | N.D | N.D | N.D | N.D | N.D | N.D |
| **7o** | 2 | 4-Br | N.D | N.D | > 100 | > 100 | N.D | N.D |
| **7p** | 1 | 4-$CH_3$ | N.D | > 100 | 74.02 ± 14.07 | > 100 | N.D | N.D |
| **7q** | 1 | 4-Cl | N.D | >100 | >100 | >100 | N.D | 75.51± 5.41 |
| **7r** | 1 | 4-Br | N.D | > 100 | 28.86 ± 9.72 | > 100 | N.D | 74.77± 6.37 |
| **7s** | 3 | H | N.D | 87.60 ± 2.23 | 27.15 ± 6.50 | 37.20 ± 7.53 | N.D | > 100 |
| **7t** | 2 | H | N.D | N.D | >100 | N.D | N.D | N.D |
| **7u** | 1 | H | N.D | > 100 | 15.27 ± 6.84 | N.D | N.D | N.D |
| **7v** | 3 | 3-Cl,5-Cl,6-Cl | N.D | N.D | > 100 | N.D | N.D | N.D |
| **7w** | 2 | 3-Cl,5-Cl,6-Cl | N.D | N.D | > 100 | > 100 | N.D | N.D |
| **7x** | 1 | 3-Cl,5-Cl,6-Cl | N.D | N.D | > 100 | N.D | N.D | N.D |
| **5-FU** | / | / | **29.27±2.60** | 45.51 ± 13.31 | 17.11 ± 2.64 | 31.96 ± 7.93 | 46.82±4.90 | > 100 |

**N.D. = not detected.**

## *2.3. Colony formation*

The colony formation rate means that the ability of a single cell-independent viability *in vitro*. Therefore, to assess the inhibition efficiency of compound **7f**, the HGC-27 cells were treated with

the candidate compound **7f** at different consistency (0, 2, 4, 8 μM). Then the comparison of the inhibition activity data (Fig. 2), manifested that compound **7f** at a concentration of 8 μM markedly inhibited colony formation by HGC-27 cells.

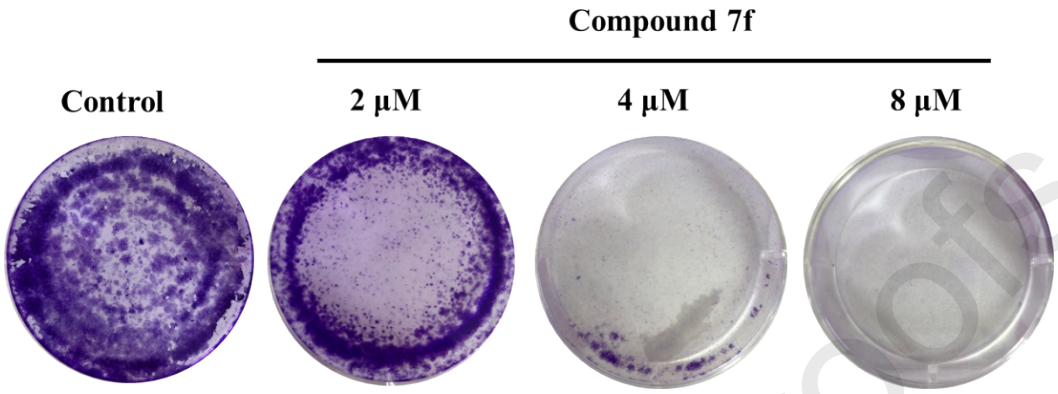


**Fig. 2.** Inhibition of colony formation on HGC-27 cells by compound **7f**.

## *2.4. Cell migration*

The wound healing assay is a laboratory technique to determine the capability of the cell migration and interactions. For this assay, the HGC-27 cells were conducted with different concentrations of **7f** (0, 4, 8 and 16 μM) for 48 h to investigate if compound **7f** could influence the migration of the cell line after an injury stimulus. As shown in Fig. 3, compared with the control group, compound **7f** inhibited migration of HGC-27 cells in a concentration-dependent manner.

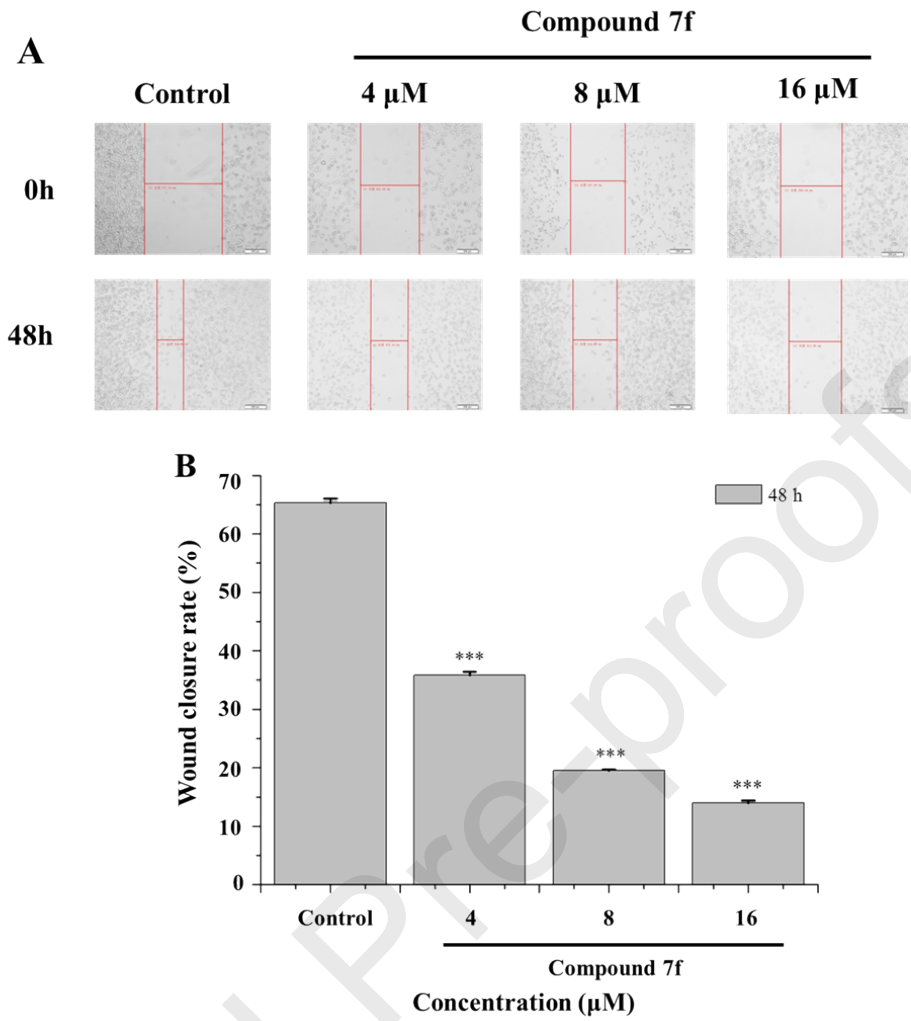


**Fig. 3.** (A) Inhibition of the migration of HGC-27 cells treated with compound **7f** for 48 h in the wound healing assay. (B) Wound closure rate was calculated as mean ± SD from three different fields. *p < 0.05, **p < 0.01 and ***p < 0.001 vs. control.

## *2.5. Cell apoptosis*

The significance of apoptosis is to building a natural balance between cell death and cell renewal in the multicellular creature. Thence, tumor cells can divide ruthlessly without programmed cell death, when there is a lack of apoptosis [34]. To define whether the antiproliferative effect of compound **7f** on tumor cells was as a result of induction of cell apoptosis, the HGC-27 cells were treated with compound **7f** at different concentrations (0, 4, 8, and 16 μM) for 48 h, Hoechst 33258 staining was used to differentiate between the apoptotic and normal cells. As shown in Fig. 4, control cells were consistently stained with Hoechst 33258 and presented round homogeneous nuclei, without morphological changes and emitted blue fluorescence. While HGC-27 cells treated with compound **7f** exhibited bright chromatin condensation, nuclear fragmentation and displayed stronger blue

fluorescence, which was a sign of apoptosis. The stain results certified that compound **7f** induced HGC-27 cells apoptosis.

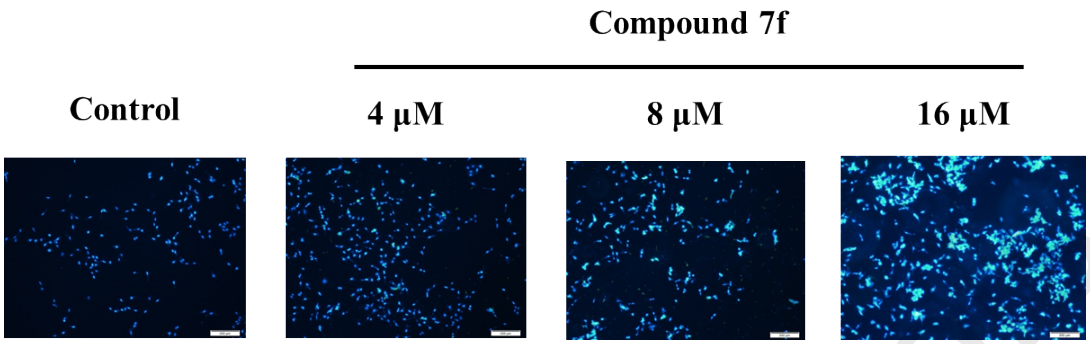


**Fig. 4.** Effect of compound **7f** treatment for 48 h on the morphology of the HGC-27 cells stained with Hoechst 33258.

Additionally, the percentage of apoptotic cells was determined by double-stained with FITC-Annexin V and PI staining by the flow cytometry. As indicated in Fig. 5, the percentage of apoptotic cells increased as the concentration of the compound increased (0 μM, 5.58%; 4 μM, 11.55%; 8 μM, 29%; 16 μM, 54.7%). The results showed that compound **7f** could induce HGC-27 cells apoptosis in a concentration-dependent manner.

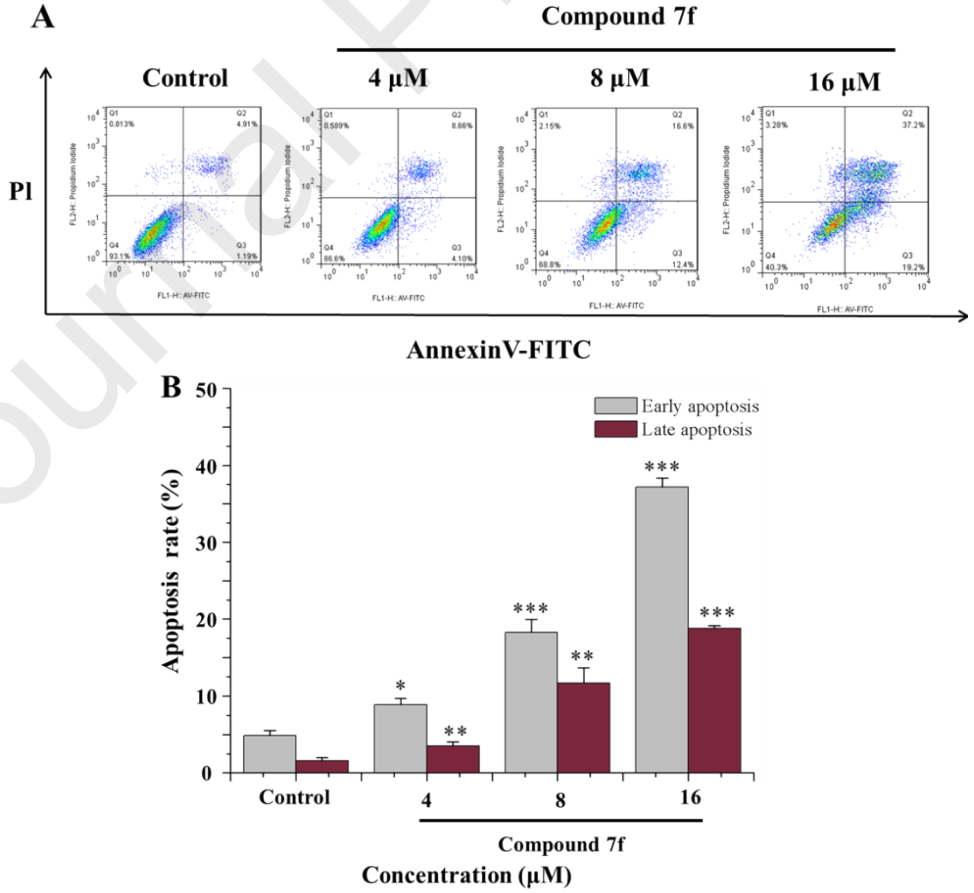

**Fig. 5.** (A) The apoptosis of HGC-27 cells was induced by compound **7f** for 48 h in a concentration-dependent manner. (B) Flow cytometry analysis of the percentage of early apoptosis and late apoptosis in triplicate and repeated three times. *$p < 0.05$, **$p < 0.01$ and ***$p < 0.001$ vs. control.

### *2.6. Cell cycle distribution*

Besides apoptosis, inducing cell cycle arrest are an important means to control growth and development of cancer cells [35]. Cell-cycle dysregulation is an important feature of tumor cells [36]. To investigate the possible significance of cell cycle arrest in the HGC-27 cell death induced by compound **7f**, cell cycle proportion was measured by flow cytometry. HGC-27 cells were treated with different concentrations of compound **7f** (0, 4, 8 and 16 μM) for 48 h and stained with propidium iodide (PI), to detect cell cycle distribution in the different phases by the flow cytometry analysis. As given in Fig. 6, with the increase of drug concentration, the percentage of cells in G2 phase increased. Compared with the control group, the percentage of cells in S phase change of the drug group showed a tendency to decrease. The experimental results indicated that HGC-27 cells proliferation were suppressed mainly through induction of G2/M cell cycle arrest under the inhibiting effect of compound **7f** in a significant concentration-dependent manner.

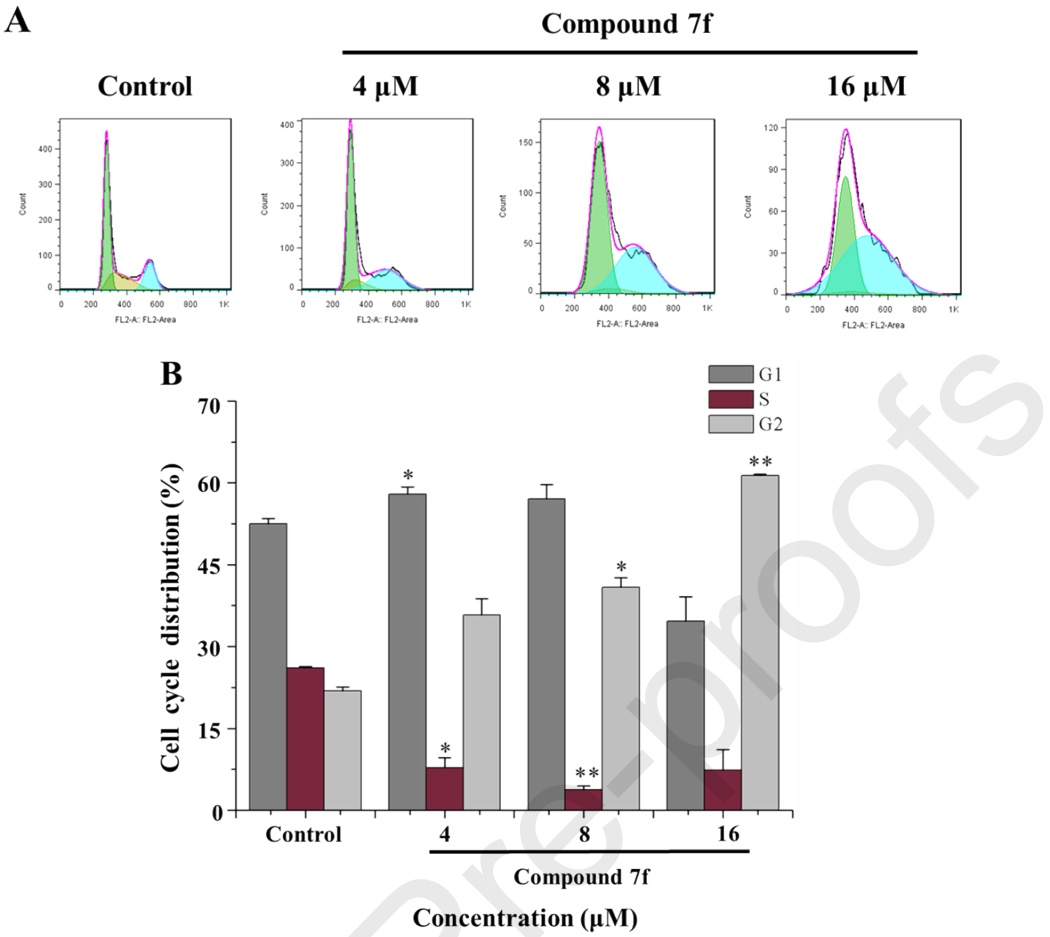


**Fig. 6.** Flow cytometry analysis of cell cycle distribution for HGC-27 cells treated with compound **7f** for 48 h. (A) Representative photographs from three independent experiments were showed. (B) Cell cycle proportion are the mean ± SD from three independent experiments. *p<0.05, **p<0.01 vs control.

### *2.7. Microtubules disarrangement*

Microtubule network perturbation can cause subsequent mitotic arrest [37]. To investigate the effects of compound **7f** on the cellular microtubule network in HGC-27 cells, in-vitro tubulin morphological analysis was determined with immunofluorescence staining via confocal microscopy. As shown in Fig. 7, in the negative control, the majority of HGC-27 cells displayed the normal distribution of microtubules. However, disordered microtubule distribution was observed around the cells after treatment with compound **7f**. Tubulin appeared agregated and disappeared in the presence of compound **7f**. 64 μM compound **7f** had the most severe effect on microtubules organization, the network almost completely disappeared. What's more, according to the results of cell apoptosis analysis and cell cycle analysis, it was speculated that compound **7f** inhibited the assembly of intracellular tubulin and disrupted microtubule dynamic, thereby arresting cells in

G2/M phase, eventually cancer cells underwent apoptosis [21-23,35].

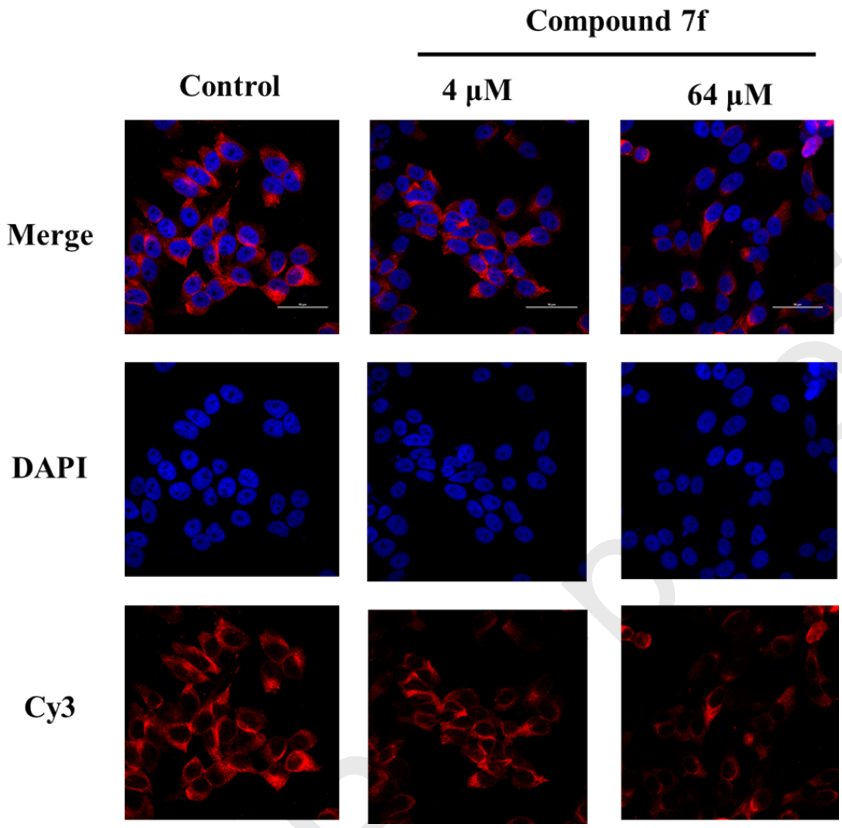


**Fig. 7.** Cy3 proliferation of HGC-27 cells cells treated with compound **7f** at 0, 4 and 64 μM for 48 h, respectively. HGC-27 cells were treated as indicated and stained for Cy3 incorporation (red) or DAPI (blue) to highlight nuclei, and the red and blue images were merged.

### *2.8. Docking studies with tubulin*

The structure and ligand-based collaborative method is being applied to determine the relationship between structure and its biological activity. Tubulin has been confirmed as a new significant anti-cancer drug target [29]. To get a deeper insight into the inhibition of HGC-27 cells by the screened compound **7f** from for ligand-protein interactions, we conducted the molecular docking simulation with the crystal structure of the DAMA–colchicine–tubulin complex (Protein Data Bank (PDB) ID: 1SA0). And the docking studies for reference drug (colchicine) be carried out as comparison. As illustrated in Fig. 8, compound **7f** occupied the colchicine binding site on tubulin, the binding site existed between the α1-tubulin and β1-tubulin subunit (Fig. 8A). Furthermore, docking simulations demonstrated that compound **7f** formed strong interactions with the catalytically active residues SER-140, GLY-146, THR-145 and ASN-101 via hydrogen-bonding. A hydrogen bond was formed

between the OH of SER-140 and oxygen atom of A-ring C5 on flavonoid structure of compound **7f**. A hydrogen bond was formed between the $NH_2$ of GLY-146 and oxygen atom of A-ring C6 on flavonoid structure of compound **7f**. Similarly, the $NH_2$ of ASN-101 formed a hydrogen bonds with the oxygen atom of C-ring O1 on flavonoid structure of compound **7f**. In addition, the $NH_2$ of THR-145 formed two additional hydrogen bonds with the two oxygen atoms of A-ring C7 and A-ring C6 on flavonoid structure of compound **7f**, respectively (Fig. 8B). Simultaneously. the colchicine binds well in the colchicine-binding domain at the α/β-tubulin interface (Fig. 8C). Moreover, a hydrogen bond was formed between the $NH_2$ of ASN-206 and oxygen atom of one of the methoxy groups on colchicine. And the $NH_2$ of ASN-179 formed a hydrogen bonds with the oxygen atom of amide bond carbonyl (Fig. 8D). The docking studies results showed that both compound 7f and the tubulin inhibitor colchicine binds well in the colchicine-binding domain at the α/β-tubulin interface, and formed a hydrogen bonds with the $NH_2$ of amino acid residues at the methoxy atom positions in a similar manner, which various hydrogen-bonding interactions appear to play a key role in the binding mode.

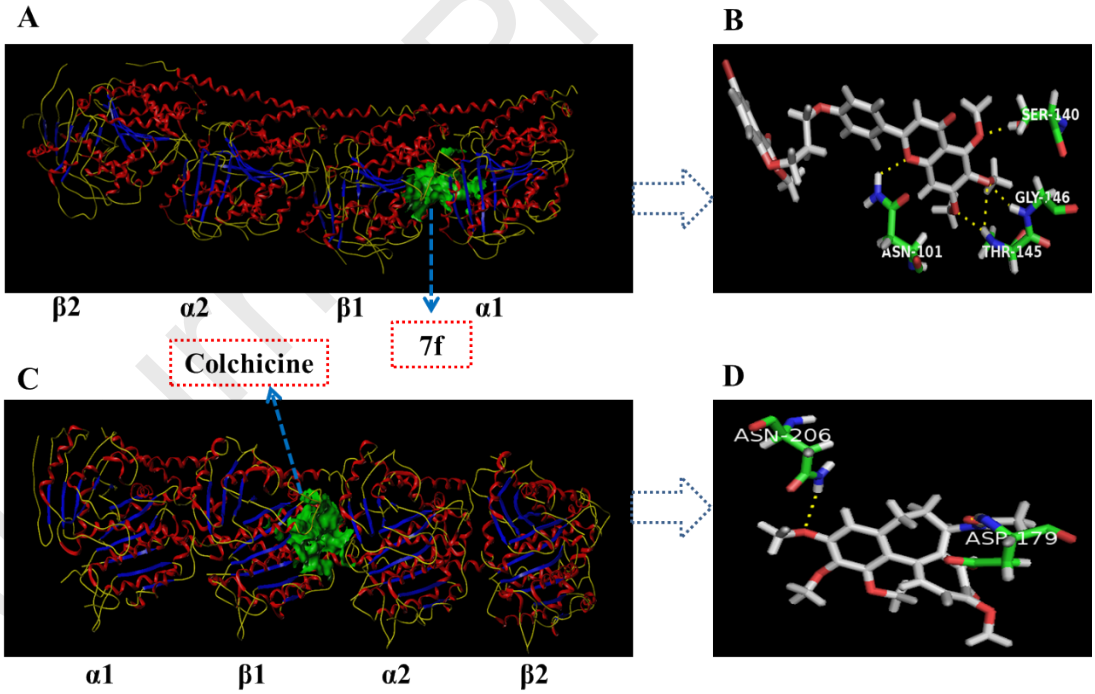


**Fig. 8.** (A) Structure of tubulin in complex with compound **7f**. (B) Hydrogen bonding interactions were displayed in yellow dashed lines. (C) Structure of tubulin in complex with colchicine. (D) Hydrogen bonding interactions were displayed in yellow dashed lines. Docking mode of compound **7f** and colchicine with the colchicine binding domain of tubulin (PDB code: 1SA0). The figures were engendered using PyMOL (http://www.pymol.org/).

### *2.9. Lactate level*

Lactate usually as a bio-marker and even as a therapeutic target [38]. From a metabolic standpoint, the most distinctive feature of cancer cells is enhanced lactate production due to the increased glycolytic activity which correlates with high glucose uptake, regardless of oxygen availability [39,40]. Studies have shown that, on one hand, proliferating cancer cells can enhance the production of lactic acid. On the other hand, the lactate exported to the extracellular space contributes to the acidification of micro-environment and remodeling of extracellular-matrix promoting tumor dissemination, and can also be taken up by neighboring cells and used as a metabolic fuel enhancing cell survival and proliferation [41]. Thence, to examine the ability of compound **7f** to suppress generation of lactic acid in cancer cells, the HGC-27 cell were cultured with various concentrations (0, 4, 8 and 16 μM) of compound **7f**, and then treated followed the steps in the lactic acid test kit. As summarized in Fig. 9, the lactic acid content of the cell culture medium showed a decreasing trend as the concentration of the target compound was increased, demonstrating that the target compound **7f** restrained the production of lactate in a manner of concentration dependence.

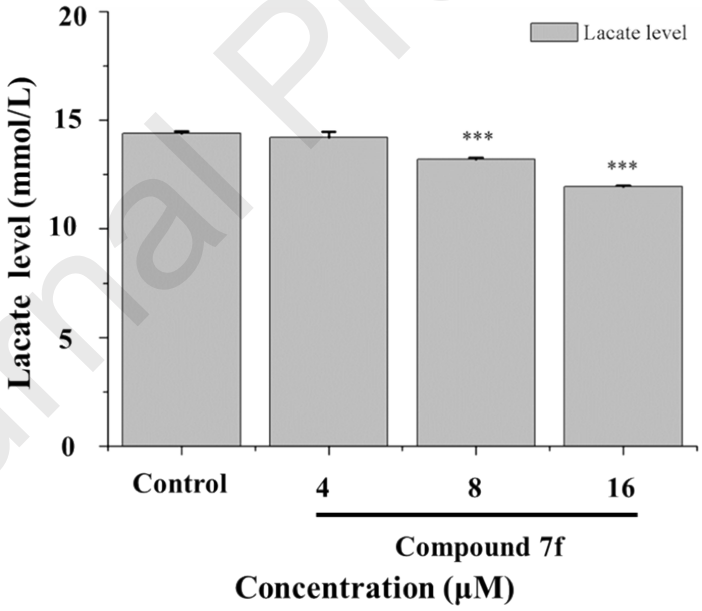


**Fig. 9.** Inhibition of lactate level of HGC-27 cells treated with compound 7f in the lactic acid test kit in triplicate and repeated three times. ***p<0.001 vs control.

### *2.10. Effects on glycolysis related proteins*

Tumor hypoxia is a common characteristic of many solid tumors [42]. Hypoxia-inducible factor 1 (HIF-1) is the critical transcription factor in the regulation of hypoxia. HIF-1 is closely related to the occurrence and development of tumors, such as angiogenesis, glycolysis, metastasis, cell

survival and apoptosis. Hexokinase (HK), pyruvate kinase (PK) and phosphofructokinase (PFK) are the key rate-limiting enzyme in glycolysis, and also are the target gene of HIF-1α regulation [43-45]. Additionally, HIF-1α functions as the key regulator in the process of angiogenesis via the activation of HIF-1α target genes such as VEGF [46]. So far, accumulating evidence concerns flavonoids as HIF-1α inhibitors for drug therapy [47,48]. Corresponding research have manifested that ASA and SA inhibited purified PFK due to the modulation of the enzyme quaternary structure [33]. TMP is considered to be an important pharmacophoric point with tubulin binding for CBSIs. Hence, 5,6,7-trimethoxy flavonoid salicylate derivatives were designed by the joining of three important pharmacophores (TMP, flavonoid, and SA) according to the combination principle. The aim was to screen out compounds that simultaneously inhibited tumor glycolysis, established blood vessels and angiogenesis, completely cut off the energy source of tumor cells to accelerate tumor cell death. To investigate whether compound **7f** could affect the expression levels of the aforementioned proteins, correspondent western blot assays were conducted, and subsequent results were shown in Fig. 10. Compound **7f** down-regulated the expression of HIF-1α under hypoxic conditions, which was consistent with design ideas of 5,6,7-trimethoxy flavonoid salicylate derivatives. What's more, compound **7f** down-regulated the expression of VEGF, PFKM and PKM2 protein apart from HK-2 in normoxia conditions. These results are basically consistent with the goals we expect to design, but the specific mechanism of how compound **7f** acts on multiple related proteins in HGC-27 cell line needs further in-depth mechanistic studies.

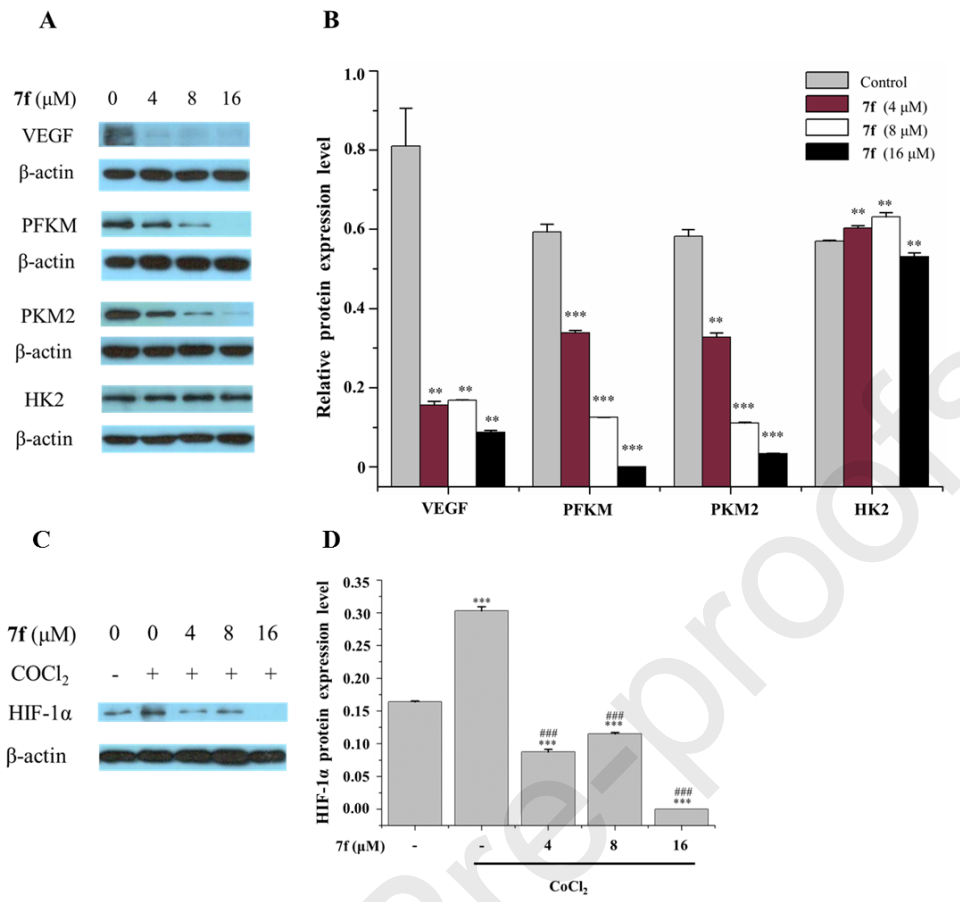


**Fig. 10.** HIF-1α, VEGF, PFKM, PKM2 and HK2 expression was detected by Western blot analysis. (A) The effect of compound **7f** treatment on the expression of VEGF, PFKM, PKM2 and HK2 under normoxic conditions. (B) Quantification of the Western blot result in Fig.10A was conducted by calculating the ratio of the value to the control group. (C) $CoCl_2$ hypoxia-mimicking conditions and serum starvation (0.1% FBS) stimulated the expression of HIF-1α. The effect of compound **7f** treatment on the expression of HIF-1α under hypoxic conditions. (D) Quantification of the Western blot result in Fig.10C was conducted by calculating the ratio of the value to the control group. All the data were confirmed by three repeated tests. *$p < 0.05$; **$p < 0.01$; ***$p < 0.001$ vs. control. $^{###}p < 0.001$ vs. $CoCl_2$ without compound **7f**.

## 3. Conclusion

Up till now, 24 novel trimethoxy flavonoid salicylate derivatives were designed and synthesized entirely and evaluated their cytotoxicity against five human cancer cell lines (MGC-803, HCT-116, HGC-27, SGC-7901 and BEL-7402) and a normal human gastric epithelial cell line (GES-1). According to the preliminary activity evaluation results, compound **7f** seemed to be the most prospective agents against the HGC-27 cell line. Subsequent the colony formation assay and wound healing assay indicated that compound **7f** effectively decreased the HGC-27 cell colony formation

and migration. Besides that, the Hoechst 33258 staining assay and flow cytometry also showed that compound **7f** induced the HGC-27 cells apoptosis, while it arrested HGC-27 cells in the G2/M phase in a concentration-dependent manner. What's more, the immunofluorescence staining analysis and molecular docking simulation exhibited that compound **7f** bound with the tubulin of cancer cells and destroyed the microtubule network which could cause subsequent mitotic arrest. Finally, the lactate measurements and western blot analysis findings revealed that compound **7f** reduced the production of lactic acid possibly by down-regulateing the expression of the glycolysis-related proteins (HIF-1α, PFKM and PKM2). In addition, compound **7f** decreased the level of angiogenesis-related proteins VEGF, suggesting that compound **7f** might inhibit the tumor angiogenesis. Taken together, compound **7f** as a representative compound possessed a good anti-tumor effect. And our research might provide a new idea for design in gastric cancer medical drug. However, the specific mechanism of action of compound **7f** still needs further research.

## 4. Experimental protocol

### *4.1. Chemicals and reagents*

All the starting materials and reagents (reagent grade) were purchased from commercial sources unless otherwise and used without further purification. Thin-layer chromatography (TLC) was run on the silica gel 60 F254 plates and visualized under UV light at 254 nm or 365 nm, which were used to monitor reaction's progress. The concentration of solutions from reactions and extractions in a rotary evaporator below 60 °C at reduced pressure. Separation of the compounds by flash column chromatography was carried out with silica gel (200 mesh size). Melting points (uncorrected) were measured with an electrothermal digital melting point apparatus (Thermo Fisher Scientific). ESI mass spectra were measured on a mass spectrometer (Bruker) in the indicated solvents (DHB as a matrix). NMR spectra were carried out on a spectrometer (Bruker) at 400 MHz in the indicated solvents (TMS as an internal standard): the values of the chemical shifts were expressed in δ values (ppm) and the coupling constants (J) in Hz.

#### *4.1.1. General procedure for the synthesis of 2-(4-hydroxy-phenyl)-5,6,7-trimethoxy-chromen-4-one (compound **3**)*

To a solution of 3,4,5-trimethoxy-phenol (**1**) (0.020 mol) in dichloromethane (100 mL), chloroacetyl chloride (0.024 mol) and a catalytic amount of aluminum trichloride were added,

followed by heating at 40 °C for 1.5 h with calcium chloride drying device，and monitored by TLC. After refrigeration, filtration, washing and drying, obtaining a flaky white precipitate of 6-Hydroxy-2,3,4-trimethoxy-benzoyl chloride (**2**) was obtained. Para-hydroxybenzaldehyde (0.016 mol) and intermediate **2** (0.013 mol) were added together to a stirred solution of 5 mL 95% ethanol, then 10% NaOH (aq.) solution was added dropwise into the solution for 24 h at RT. Finally, acidification with 10% HCl (aq.) gave a crude product, which was filtered off and purified by recrystallization from 95% ethanol to give compound **3** as a yellow powder.

*4.1.2. General procedure for the synthesis of compounds **4a-4c***

To a stirring solution of compound **3** (0.5 mol) in acetone (50 mL), a certain amount of $K_2CO_3$ at room temperature and 1, 2 dibromoethane (2.0 mol) were added dropwise to the reaction mixture, refluxed at 60 °C for 9 h (the reaction was monitored by TLC). After the completion of the reaction, the solvent was evaporated under vacuum. The residue was purified by flash column chromatography on silica gel, eluted with dichloromethane/methanol (v/v, 100 : 1) to get the intermediate **4a** as a yellow powder. Compounds **4b** and **4c** were prepared in the same way, except that 1, 3 dibromopropane and 1, 4 dibromobutane were used as the reactants, respectively.

*4.1.2.1. 2-[4-(2-Bromo-ethoxy)-phenyl]-5,6,7-trimethoxy-chromen-4-one(compound **4a**)*

Compound **4a** was obtained as yellow solid; yield: 85.5%; m.p: 143.6-144.2 °C; $^1$H NMR (400 MHz, $CDCl_3$): δ (ppm) 7.88 (d, *J* = 8.6 Hz, 2H), 7.01 (d, *J* = 8.6 Hz, 2H), 6.79 (s, 1H), 6.59 (s, 1H), 4.39 (t, *J* = 6.2 Hz, 2H), 4.30 (s, 3H), 4.03 (s, 3H), 3.87 (s, 3H), 3.71 (t, *J* = 6.2 Hz, 2H). MS (ESI) m/z: 435.196 $[M + H]^+$, calcd. for $C_{20}H_{19}BrO_6$ 434.037.

*4.1.2.2. 2-[4-(3-Bromo-propoxy)-phenyl]-5,6,7-trimethoxy-chromen-4-one(compound **4b**)*

Compound **4b** was obtained as yellow solid; yield: 82.7%; m.p: 117.0-117.9 °C; $^1$H NMR (400 MHz, CDCl3): δ (ppm) 7.89 – 7.80 (m, 2H), 7.02 – 6.95 (m, 2H), 6.77 (s, 1H), 6.57 (s, 1H), 4.28 (s, 3H), 4.23 – 4.15 (m, 2H), 4.00 (s, 3H), 3.86 (d, *J* = 9.8 Hz, 3H), 3.64 (t, *J* = 6.4 Hz, 2H), 2.44 – 2.29 (m, 2H). MS (ESI) m/z: 449.228 $[M + H]^+$, calcd. for $C_{21}H_{21}BrO_6$ 448.052.

*4.1.2.3. 2-[4-(4-Bromo-butoxy)-phenyl]-5,6,7-trimethoxy-chromen-4-one(compound **4c**)*

Compound **4c** was obtained as yellow solid; yield: 79.7%; m.p: 117.2-118.2 °C; $^1$H NMR (400 MHz,

$CDCl_3$): δ (ppm) 7.92 – 7.80 (m, 2H), 7.04 – 6.93 (m, 2H), 6.79 (s, 1H), 6.59 (d, *J* = 2.4 Hz, 1H), 4.30 (d, *J* = 2.6 Hz, 3H), 4.10 (dd, *J* = 7.6, 4.1 Hz, 2H), 4.02 (s, 3H), 3.87 (d, *J* = 2.5 Hz, 3H), 3.54 (dd, *J* = 8.5, 4.4 Hz, 2H), 2.16 – 1.98 (m, 4H). MS (ESI) m/z: 463.300 $[M + H]^+$, calcd. for $C_{22}H_{23}BrO_6$ 462.068.

### *4.1.3. General procedure for the synthesis of intermediates **6a-6h***

Methyl 4-bromosalicylate (1 mol) was dissolved in methanol (25 mL), and thionyl chloride was added dropwise under ice-cooling, after 10 min, The mixture was stirred at 65 °C for 48 h. and monitored by TLC. After the reaction was completed, excess methanol was evaporated, the residue was extracted with ethyl acetate and aqueous sodium carbonate, and the organic phase was added to anhydrous sodium sulfate and concentrated to obtain intermediate **6a**.

The compounds **6b–6h** were prepared analogously.

### *4.1.4. General procedure for the synthesis of compounds **7a–7x.***

The intermediates **6a** and **4a** were dissolved in acetone (30 mL), and a catalytic amount of anhydrous potassium carbonate was added to this solution at 60 °C for 48 h (the reaction was monitored by TLC). After completion of the reaction, the solvent was evaporated, the residue was extracted with ethyl acetate and water, the organic phase was treated with anhydrous sodium sulfate, and then concentrated. The final target product **7a** was purified by flash column chromatography on silica gel, and eluted with a solution of methanol and dichloromethane (v/v, 1 : 100) and recrystallized from anhydrous ethanol.

Compounds **7b–7x** were prepared similarly.

#### ***4.1.4.1.*** *5-Methyl-2-{4-[4-(5,6,7-trimethoxy-4-oxo-4H-chromen-2-yl)-phenoxy]-butoxy}-benzoic acid methyl ester (compound **7a**)*

Compound **7a** was obtained as yellow solid; yield: 88.9%; m.p: 113.5-114.8 °C; $^1$H NMR (400 MHz, $CDCl_3$): δ (ppm) 7.86 (d, *J* = 8.8 Hz, 2H), 7.64 (d, *J* = 1.9 Hz, 1H), 7.27 (d, *J* = 2.2 Hz, 1H), 7.00 (d, *J* = 8.8 Hz, 2H), 6.91 (d, *J* = 8.5 Hz, 1H), 6.79 (s, 1H), 6.59 (s, 1H), 4.30 (s, 3H), 4.14 (q, *J* = 5.6 Hz, 4H), 4.02 (s, 3H), 3.91 (s, 3H), 3.86 (s, 3H), 2.34 (s, 3H), 2.13 – 2.03 (m, 4H). $^{13}$C NMR (101 MHz, $CDCl_3$): δ (ppm) 180.73 (s), 166.90 (s), 163.79 (s), 161.39 (s), 160.19 (s), 156.44 (s), 151.60 (s), 146.55 (s), 136.58 (s), 133.95 (s), 132.96 (s), 131.94 (s), 129.60 (s), 125.10 (s), 120.03 (s), 114.91 (s), 113.37 (s), 111.56 (s), 107.30 (s), 90.54 (s), 68.54 (s), 67.63 (s), 62.41 (s), 61.62 (s),

56.60 (s), 51.87 (s), 25.94 (d, *J* = 2.1 Hz), 20.28 (s). MS (ESI) m/z: 549.11 $[M + H]^+$, calcd. for $C_{31}H_{32}O_9$ 548.20.

*4.1.4.2. 5-Chloro-2-{4-[4-(5,6,7-trimethoxy-4-oxo-4H-chromen-2-yl)-phenoxy]-butoxy}-benzoic acid methyl ester (compound **7b**)*

Compound **7b** was obtained as yellow solid; yield: 68.2%; m.p: 136.8-138.5 °C; $^1$H NMR (400 MHz, $CDCl_3$): δ (ppm) 7.86 (d, *J* = 8.8 Hz, 2H), 7.82 (d, *J* = 2.7 Hz, 1H), 7.45 (dd, *J* = 8.9, 2.7 Hz, 1H), 6.98 (dd, *J* = 15.2, 8.9 Hz, 3H), 6.80 (s, 1H), 6.60 (s, 1H), 4.30 (s, 3H), 4.16 (d, *J* = 2.9 Hz, 4H), 4.03 (s, 3H), 3.92 (s, 3H), 3.87 (s, 3H), 2.10 (s, 4H). $^{13}$C NMR (101 MHz, $CDCl_3$): δ (ppm) 180.74 (s), 165.42 (s), 163.79 (s), 161.41 (s), 160.10 (s), 157.15 (s), 151.60 (s), 146.58 (s), 136.59 (s), 133.11 (s), 132.96 (s), 131.38 (s), 125.19 (d, *J* = 2.9 Hz), 121.49 (s), 114.89 (s), 114.53 (s), 111.51 (s), 107.30 (s), 90.54 (s), 68.76 (s), 67.53 (s), 62.41 (s), 61.63 (s), 56.61 (s), 52.15 (s), 25.85 (d, *J* = 3.8 Hz). MS (ESI) m/z: 569.02 $[M + H]^+$, calcd. for $C_{30}H_{29}ClO_9$ 568.15.

*4.1.4.3. 5-Bromo-2-{4-[4-(5,6,7-trimethoxy-4-oxo-4H-chromen-2-yl)-phenoxy]-butoxy}-benzoic acid methyl ester (compound **7c**)*

Compound **7c** was obtained as yellow solid; yield: 64.8%; m.p: 137.9-139.5 °C; $^1$H NMR (400 MHz, $CDCl_3$): δ (ppm) 7.96 (d, *J* = 2.5 Hz, 1H), 7.86 (d, *J* = 8.7 Hz, 2H), 7.58 (dd, *J* = 8.8, 2.5 Hz, 1H), 6.99 (d, *J* = 8.7 Hz, 2H), 6.91 (d, *J* = 8.9 Hz, 1H), 6.80 (s, 1H), 6.60 (s, 1H), 4.30 (s, 3H), 4.15 (d, *J* = 3.4 Hz, 4H), 4.03 (s, 3H), 3.92 (s, 3H), 3.87 (s, 3H), 2.10 (s, 4H). $^{13}$C NMR (101 MHz, $CDCl_3$): δ (ppm) 180.71 (s), 165.27 (s), 163.78 (s), 161.40 (s), 160.09 (s), 157.63 (s), 151.59 (s), 146.57 (s), 136.59 (s), 136.03 (s), 134.24 (s), 132.96 (s), 125.16 (s), 121.91 (s), 114.90 (d, *J* = 3.7 Hz), 112.21 (s), 111.48 (s), 107.28 (s), 90.54 (s), 68.68 (s), 67.52 (s), 62.41 (s), 61.62 (s), 56.61 (s), 52.15 (s), 25.85 (s). MS (ESI) m/z: 612.97 $[M + H]^+$, calcd. for $C_{30}H_{29}BrO_9$ 612.10.

*4.1.4.4. 5-Methyl-2-{3-[4-(5,6,7-trimethoxy-4-oxo-4H-chromen-2-yl)-phenoxy]-propoxy}-benzoic acid methyl ester (compound **7d**)*

Compound **7d** was obtained as yellow solid; yield: 45.3%; m.p: 107.5-109.0 °C; $^1$H NMR (400 MHz, $CDCl_3$): δ (ppm) 7.86 (d, *J* = 8.8 Hz, 2H), 7.64 (d, *J* = 2.0 Hz, 1H), 7.28 (d, *J* = 1.9 Hz, 1H), 7.02 (d, *J* = 8.8 Hz, 2H), 6.93 (d, *J* = 8.5 Hz, 1H), 6.79 (s, 1H), 6.59 (s, 1H), 4.33 (t, *J* = 6.1 Hz, 2H), 4.30 (s, 3H), 4.26 (t, *J* = 5.9 Hz, 2H), 4.02 (s, 3H), 3.90 (s, 3H), 3.87 (s, 3H), 2.40 – 2.32 (m, 5H). $^{13}$C NMR (101 MHz, $CDCl_3$): δ (ppm) 180.73 (s), 166.80 (s), 163.79 (s), 161.39 (s), 160.08 (s), 156.32 (s), 151.59 (s), 146.57 (s), 136.58 (s), 133.99 (s), 132.97 (s), 131.95 (s), 129.82 (s), 125.21

(s), 120.08 (s), 114.95 (s), 113.53 (s), 111.51 (s), 107.29 (s), 90.54 (s), 65.40 (s), 64.55 (s), 62.40 (s), 61.62 (s), 56.60 (s), 51.88 (s), 29.21 (s), 20.28 (s). MS (ESI) m/z: 535.09 $[M + H]^+$, calcd. for $C_{30}H_{30}O_9$ 534.19.

*4.1.4.5. 5-Chloro-2-{3-[4-(5,6,7-trimethoxy-4-oxo-4H-chromen-2-yl)-phenoxy]-propoxy}-benzoic acid methyl ester (compound **7e**)*

Compound **7e** was obtained as yellow solid; yield: 62.8%; m.p: 154.0-154.5 °C; $^1$H NMR (400 MHz, $CDCl_3$): δ (ppm) 7.86 (d, *J* = 8.8 Hz, 2H), 7.81 (d, *J* = 2.7 Hz, 1H), 7.44 (dd, *J* = 8.9, 2.7 Hz, 1H), 7.00 (dd, *J* = 16.2, 8.9 Hz, 3H), 6.79 (s, 1H), 6.58 (s, 1H), 4.32 (t, *J* = 6.1 Hz, 2H), 4.30 (s, 3H), 4.27 (t, *J* = 5.9 Hz, 2H), 4.02 (s, 3H), 3.91 (s, 3H), 3.86 (s, 3H), 2.37 (p, *J* = 5.9 Hz, 2H). $^{13}$C NMR (101 MHz, $CDCl_3$): δ (ppm) 180.73 (s), 165.30 (s), 163.79 (s), 161.42 (s), 159.96 (s), 157.04 (s), 151.60 (s), 146.60 (s), 136.59 (s), 133.15 (s), 132.97 (s), 131.39 (s), 125.40 (s), 125.31 (s), 121.51 (s), 114.93 (s), 114.69 (s), 111.43 (s), 107.28 (s), 90.54 (s), 65.59 (s), 64.30 (s), 62.40 (s), 61.62 (s), 56.61 (s), 52.16 (s), 29.08 (s). MS (ESI) m/z: 555.11 $[M + H]^+$, calcd. for $C_{29}H_{27}ClO_9$ 554.13.

*4.1.4.6. 5-Bromo-2-{3-[4-(5,6,7-trimethoxy-4-oxo-4H-chromen-2-yl)-phenoxy]-propoxy}-benzoic acid methyl ester (compound **7f**)*

Compound **7f** was obtained as yellow solid; yield: 80.9%; m.p: 160.5-162.8 °C; $^1$H NMR (400 MHz, $CDCl_3$): δ (ppm) 7.92 (d, *J* = 2.6 Hz, 1H), 7.83 (d, *J* = 8.8 Hz, 2H), 7.55 (dd, *J* = 8.9, 2.6 Hz, 1H), 6.99 (d, *J* = 8.8 Hz, 2H), 6.90 (d, *J* = 8.9 Hz, 1H), 6.76 (s, 1H), 6.56 (s, 1H), 4.29 (t, *J* = 6.0 Hz, 2H), 4.27 (s, 3H), 4.24 (t, *J* = 5.9 Hz, 2H), 3.99 (s, 3H), 3.88 (s, 3H), 3.84 (s, 3H), 2.34 (p, *J* = 5.9 Hz, 2H). $^{13}$C NMR (101 MHz, $CDCl_3$): δ (ppm) 180.71 (s), 165.16 (s), 163.79 (s), 161.41 (s), 159.95 (s), 157.53 (s), 151.61 (s), 146.60 (s), 136.60 (s), 136.07 (s), 134.27 (s), 132.97 (s), 125.32 (s), 121.94 (s), 115.08 (s), 114.93 (s), 112.43 (s), 111.41 (s), 107.28 (s), 90.54 (s), 65.52 (s), 64.29 (s), 62.41 (s), 61.62 (s), 56.61 (s), 52.16 (s), 29.06 (s). MS (ESI) m/z: 601.76 $[M + H]^+$, calcd. for $C_{29}H_{27}BrO_9$ 598.08.

*4.1.4.7. 5-Methyl-2-{2-[4-(5,6,7-trimethoxy-4-oxo-4H-chromen-2-yl)-phenoxy]-ethoxy}-benzoic acid methyl ester (compound **7g**)*

Compound **7g** was obtained as yellow solid; yield: 63.1%; m.p: 172.5-175.6 °C; $^1$H NMR (400 MHz, $CDCl_3$): δ (ppm) 7.88 (d, *J* = 8.8 Hz, 2H), 7.65 (d, *J* = 1.8 Hz, 1H), 7.34 – 7.31 (m, 1H), 7.06 (d, *J* = 8.8 Hz, 2H), 7.00 (d, *J* = 8.4 Hz, 1H), 6.80 (s, 1H), 6.59 (s, 1H), 4.46 (d, *J* = 8.9 Hz, 4H), 4.30 (s, 3H), 4.03 (s, 3H), 3.88 (s, 3H), 3.87 (s, 3H), 2.36 (s, 3H). $^{13}$C NMR (101 MHz, $CDCl_3$): δ (ppm)

180.74 (s), 166.80 (s), 163.82 (s), 161.45 (s), 159.77 (s), 156.12 (s), 151.60 (s), 146.67 (s), 136.60 (s), 133.97 (s), 132.96 (s), 131.92 (s), 130.71 (s), 125.59 (s), 120.95 (s), 115.11 (s), 114.92 (s), 111.35 (s), 107.26 (s), 90.55 (s), 68.36 (s), 66.70 (s), 62.40 (s), 61.62 (s), 56.61 (s), 51.96 (s), 20.34 (s). MS (ESI) m/z: 521.07 $[M + H]^+$, calcd. for $C_{29}H_{28}O_9$ 520.17.

*4.1.4.8. 5-Chloro-2-{2-[4-(5,6,7-trimethoxy-4-oxo-4H-chromen-2-yl)-phenoxy]-ethoxy}-benzoic acid methyl ester (compound **7h**)*

Compound **7h** was obtained as yellow solid; yield: 67.2%; m.p: 139.0-140.5 °C; $^1$H NMR (400 MHz, $CDCl_3$): δ (ppm) 7.88 (d, *J* = 8.8 Hz, 2H), 7.82 (d, *J* = 2.7 Hz, 1H), 7.47 (dd, *J* = 8.9, 2.7 Hz, 1H), 7.05 (d, *J* = 8.8 Hz, 3H), 6.79 (s, 1H), 6.59 (s, 1H), 4.46 (s, 4H), 4.30 (s, 3H), 4.02 (s, 3H), 3.88 (s, 3H), 3.87 (s, 3H). $^{13}$C NMR (101 MHz, $CDCl_3$): δ (ppm) 180.73 (s), 165.32 (s), 163.81 (s), 161.47 (s), 159.60 (s), 156.83 (s), 151.61 (s), 146.71 (s), 136.61 (s), 133.11 (s), 132.96 (s), 131.36 (s), 126.21 (s), 125.72 (s), 122.41 (s), 115.98 (s), 115.07 (s), 111.23 (s), 107.23 (s), 90.55 (s), 68.44 (s), 66.55 (s), 62.40 (s), 61.62 (s), 56.62 (s), 52.24 (s). MS (ESI) m/z: 541.12 $[M + H]^+$, calcd. for $C_{28}H_{25}ClO_9$ 540.12.

*4.1.4.9. 5-Bromo-2-{2-[4-(5,6,7-trimethoxy-4-oxo-4H-chromen-2-yl)-phenoxy]-ethoxy}-benzoic acid methyl ester (compound **7i**)*

Compound **7i** was obtained as yellow solid; yield: 52.3%; m.p: 160.5-162.8 °C; $^1$H NMR (400 MHz, $CDCl_3$): δ (ppm) 7.96 (d, *J* = 2.6 Hz, 1H), 7.88 (d, *J* = 8.8 Hz, 2H), 7.61 (dd, *J* = 8.8, 2.6 Hz, 1H), 7.05 (d, *J* = 8.8 Hz, 2H), 7.00 (d, *J* = 8.9 Hz, 1H), 6.80 (s, 1H), 6.59 (s, 1H), 4.46 (s, 4H), 4.30 (s, 3H), 4.03 (s, 3H), 3.88 (s, 3H), 3.87 (s, 3H). $^{13}$C NMR (101 MHz, $CDCl_3$): δ (ppm) 180.70 (s), 165.19 (s), 163.81 (s), 161.46 (s), 159.59 (s), 157.33 (s), 151.64 (s), 146.73 (s), 136.64 (s), 136.02 (s), 134.25 (s), 132.94 (s), 125.76 (s), 122.88 (s), 116.35 (s), 115.09 (s), 113.31 (s), 111.18 (s), 107.25 (s), 90.54 (s), 68.37 (s), 66.55 (s), 62.39 (s), 61.61 (s), 56.61 (s), 52.22 (s), 29.69 (s). MS (ESI) m/z: 584.94 $[M + H]^+$, calcd. for $C_{28}H_{25}BrO_9$ 584.07.

*4.1.4.10. 4-Methyl-2-{4-[4-(5,6,7-trimethoxy-4-oxo-4H-chromen-2-yl)-phenoxy]-butoxy}-benzoic acid methyl ester (compound **7j**)*

Compound **7j** was obtained as yellow solid; yield: 58.0%; m.p: 109.0-112.2°C; $^1$H NMR (400 MHz, $CDCl_3$): δ (ppm) 7.82 (d, *J* = 8.1 Hz, 2H), 7.72 (d, *J* = 7.8 Hz, 1H), 6.96 (d, *J* = 8.1 Hz, 2H), 6.78 (t, *J* = 8.7 Hz, 3H), 6.55 (s, 1H), 4.26 (s, 3H), 4.12 (d, *J* = 4.8 Hz, 4H), 3.98 (s, 3H), 3.86 (s, 3H), 3.82 (s, 3H), 2.37 (s, 3H), 2.06 (s, 4H). $^{13}$C NMR (101 MHz, $CDCl_3$): δ (ppm) 180.72 (s), 166.62

(s), 163.78 (s), 161.39 (s), 160.19 (s), 158.75 (s), 151.59 (s), 146.55 (s), 144.52 (s), 136.58 (s), 132.96 (s), 131.86 (s), 125.10 (s), 121.05 (s), 117.23 (s), 114.91 (s), 113.93 (s), 111.54 (s), 107.29 (s), 90.54 (s), 68.25 (s), 67.62 (s), 62.40 (s), 61.61 (s), 56.60 (s), 51.72 (s), 25.93 (s), 21.90 (s). MS (ESI) m/z: 549.06 $[M + H]^+$, calcd. for $C_{31}H_{32}O_9$ 548.20.

*4.1.4.11. 4-Chloro-2-{4-[4-(5,6,7-trimethoxy-4-oxo-4H-chromen-2-yl)-phenoxy]-butoxy}-benzoic acid methyl ester (compound **7k**)*

Compound **7k** was obtained as yellow solid; yield: 73.7%; m.p: 123.5-125.5 °C; $^1$H NMR (400 MHz, $CDCl_3$): δ (ppm) 7.86 (d, *J* = 8.8 Hz, 2H), 7.83 – 7.79 (m, 1H), 7.00 (dd, *J* = 7.5, 4.1 Hz, 4H), 6.80 (s, 1H), 6.59 (s, 1H), 4.30 (s, 3H), 4.16 (d, *J* = 1.6 Hz, 4H), 4.02 (s, 3H), 3.91 (s, 3H), 3.87 (s, 3H), 2.11 (s, 4H). $^{13}$C NMR (101 MHz, $CDCl_3$): δ (ppm) 180.76 (s), 165.81 (s), 163.80 (s), 161.41 (s), 160.10 (s), 159.23 (s), 151.62 (s), 146.58 (s), 139.32 (s), 136.60 (s), 132.97 (s), 132.86 (s), 125.18 (s), 120.43 (s), 118.56 (s), 114.90 (s), 113.64 (s), 111.54 (s), 107.31 (s), 90.54 (s), 68.66 (s), 67.50 (s), 62.42 (s), 61.63 (s), 56.61 (s), 53.45 (s), 52.01 (s), 25.82 (d, *J* = 3.8 Hz). MS (ESI) m/z: 568.96 $[M + H]^+$, calcd. for $C_{30}H_{29}ClO_9$ 568.15.

*4.1.4.12. 4-Bromo-2-{4-[4-(5,6,7-trimethoxy-4-oxo-4H-chromen-2-yl)-phenoxy]-butoxy}-benzoic acid methyl ester (compound **7l**)*

Compound **7l** was obtained as yellow solid; yield: 58.2%; m.p: 138.0-140.0 °C; $^1$H NMR (400 MHz, $CDCl_3$): δ (ppm) 7.86 (d, *J* = 8.8 Hz, 2H), 7.74 – 7.70 (m, 1H), 7.18 – 7.15 (m, 2H), 7.00 (d, *J* = 8.8 Hz, 2H), 6.79 (s, 1H), 6.59 (s, 1H), 4.30 (s, 3H), 4.16 (d, *J* = 1.3 Hz, 4H), 4.02 (s, 3H), 3.90 (s, 3H), 3.87 (s, 3H), 2.10 (s, 4H). $^{13}$C NMR (101 MHz, $CDCl_3$): δ (ppm) 180.73 (s), 165.90 (s), 163.79 (s), 161.40 (s), 160.10 (s), 159.10 (s), 151.61 (s), 146.57 (s), 136.59 (s), 132.97 (s), 127.63 (s), 125.18 (s), 123.42 (s), 119.03 (s), 116.60 (s), 114.90 (s), 111.51 (s), 107.30 (s), 90.54 (s), 68.69 (s), 67.49 (s), 62.42 (s), 61.63 (s), 56.61 (s), 52.02 (s), 25.80 (s). MS (ESI) m/z: 613.03 $[M + H]^+$, calcd. for $C_{30}H_{29}BrO_9$ 612.10.

*4.1.4.13. 4-Methyl-2-{3-[4-(5,6,7-trimethoxy-4-oxo-4H-chromen-2-yl)-phenoxy]-propoxy}-benzoic acid methyl ester (compound **7m**)*

Compound **7m** was obtained as yellow solid; yield: 83.5%; m.p: 105.5-109.0 °C; $^1$H NMR (400 MHz, $CDCl_3$): δ (ppm) 7.81 (d, *J* = 8.2 Hz, 2H), 7.72 (d, *J* = 7.9 Hz, 1H), 6.99 (d, *J* = 8.3 Hz, 2H), 6.79 (d, *J* = 7.4 Hz, 2H), 6.75 (s, 1H), 6.54 (s, 1H), 4.30 (t, *J* = 6.0 Hz, 2H), 4.25 (s, 3H), 4.23 (d, *J* = 5.8 Hz, 2H), 3.98 (s, 3H), 3.85 (s, 3H), 3.81 (d, *J* = 7.0 Hz, 3H), 2.36 (s, 3H), 2.35 – 2.29 (m, 2H).

$^{13}$C NMR (101 MHz, $CDCl_3$): δ (ppm) 180.75 (s), 166.54 (s), 163.79 (s), 161.42 (s), 160.08 (s), 158.63 (s), 151.58 (s), 146.57 (s), 144.60 (s), 136.58 (s), 132.98 (s), 131.86 (s), 125.20 (s), 121.22 (s), 117.24 (s), 114.96 (s), 114.06 (s), 111.55 (s), 107.28 (s), 90.55 (s), 65.09 (s), 64.52 (s), 62.39 (s), 61.62 (s), 56.61 (s), 51.75 (s), 29.20 (s), 21.88 (s). MS (ESI) m/z: 535.09 $[M + H]^+$, calcd. for $C_{30}H_{30}O_9$ 534.19.

*4.1.4.14. 4-Chloro-2-{3-[4-(5,6,7-trimethoxy-4-oxo-4H-chromen-2-yl)-phenoxy]-propoxy}-benzoic acid methyl ester (compound **7n**)*

Compound **7n** was obtained as yellow solid; yield: 76.7%; m.p: 120.0-121.5 °C; $^1$H NMR (400 MHz, $CDCl_3$): δ (ppm) 7.86 (d, *J* = 8.8 Hz, 2H), 7.80 (d, *J* = 8.3 Hz, 1H), 7.01 (dd, *J* = 8.4, 5.4 Hz, 4H), 6.79 (s, 1H), 6.58 (s, 1H), 4.33 (t, *J* = 6.0 Hz, 2H), 4.29 (s, 3H), 4.27 (d, *J* = 5.9 Hz, 2H), 4.02 (s, 3H), 3.90 (s, 3H), 3.86 (s, 3H), 2.37 (dd, *J* = 11.9, 6.0 Hz, 2H). $^{13}$C NMR (101 MHz, $CDCl_3$): δ (ppm) 180.75 (s), 165.69 (s), 163.80 (s), 161.42 (s), 159.95 (s), 159.11 (s), 151.61 (s), 146.60 (s), 139.36 (s), 136.59 (s), 132.98 (s), 132.87 (s), 125.32 (s), 120.59 (s), 118.56 (s), 114.93 (s), 113.76 (s), 111.47 (s), 107.29 (s), 90.54 (s), 65.44 (s), 64.23 (s), 62.41 (s), 61.63 (s), 56.61 (s), 52.01 (s), 29.00 (s). MS (ESI) m/z: 555.00 $[M + H]^+$, calcd. for $C_{29}H_{27}ClO_9$ 554.13.

*4.1.4.15. 4-Bromo-2-{3-[4-(5,6,7-trimethoxy-4-oxo-4H-chromen-2-yl)-phenoxy]-propoxy}-benzoic acid methyl ester (compound **7o**)*

Compound **7o** was obtained as yellow solid; yield: 59.5%; m.p: 132.2-134.2 °C; $^1$H NMR (400 MHz, $CDCl_3$): δ (ppm) 7.86 (d, *J* = 8.8 Hz, 2H), 7.72 (d, *J* = 8.3 Hz, 1H), 7.20 – 7.15 (m, 2H), 7.02 (d, *J* = 8.8 Hz, 2H), 6.79 (s, 1H), 6.58 (s, 1H), 4.32 (t, *J* = 6.0 Hz, 2H), 4.29 (s, 3H), 4.27 (d, *J* = 5.9 Hz, 2H), 4.02 (s, 3H), 3.89 (s, 3H), 3.86 (s, 3H), 2.38 (p, *J* = 5.9 Hz, 2H). $^{13}$C NMR (101 MHz, $CDCl_3$): δ (ppm) 180.71 (s), 165.78 (s), 163.79 (s), 161.40 (s), 159.94 (s), 158.98 (s), 151.60 (s), 146.60 (s), 136.58 (s), 132.96 (d, *J* = 2.6 Hz), 127.66 (s), 125.32 (s), 123.58 (s), 119.04 (s), 116.72 (s), 114.93 (s), 111.43 (s), 107.27 (s), 90.54 (s), 65.48 (s), 64.22 (s), 62.40 (s), 61.62 (s), 56.61 (s), 52.02 (s), 29.00 (s). MS (ESI) m/z: 599.11 $[M + H]^+$, calcd. for $C_{29}H_{27}BrO_9$ 598.08.

*4.1.4.16. 4-Methyl-2-{2-[4-(5,6,7-trimethoxy-4-oxo-4H-chromen-2-yl)-phenoxy]-ethoxy}-benzoic acid methyl ester (compound **7p**)*

Compound **7p** was obtained as yellow solid; yield: 71.7%; m.p: 178-181.5 °C; $^1$H NMR (400 MHz, $CDCl_3$): δ (ppm) 7.84 (d, *J* = 8.0 Hz, 2H), 7.73 (d, *J* = 7.7 Hz, 1H), 7.03 (d, *J* = 8.1 Hz, 2H), 6.85 (d, *J* = 9.3 Hz, 2H), 6.76 (s, 1H), 6.55 (s, 1H), 4.43 (s, 4H), 4.26 (s, 3H), 3.98 (s, 3H), 3.83 (s, 6H),

2.39 (s, 3H). $^{13}$C NMR (101 MHz, $CDCl_3$): δ (ppm) 180.78 (s), 166.57 (s), 163.83 (s), 161.48 (s), 159.76 (s), 158.40 (s), 151.61 (s), 146.68 (s), 144.57 (s), 136.59 (s), 132.98 (s), 131.83 (s), 125.60 (s), 121.99 (s), 118.07 (s), 115.30 (s), 115.12 (s), 111.41 (s), 107.26 (s), 90.55 (s), 67.96 (s), 66.67 (s), 62.39 (s), 61.62 (s), 56.62 (s), 51.83 (s), 21.84 (s). MS (ESI) m/z: 521.07 $[M + H]^+$, calcd. for $C_{29}H_{28}O_9$ 520.17.

*4.1.4.17. 4-Chloro-2-{2-[4-(5,6,7-trimethoxy-4-oxo-4H-chromen-2-yl)-phenoxy]-ethoxy}-benzoic acid methyl ester (compound **7q**)*

Compound **7q** was obtained as yellow solid; yield: 74.9%; m.p: 148.5-150.5 °C; $^1$H NMR (400 MHz, $CDCl_3$): δ (ppm) 7.88 (d, $J$ = 8.8 Hz, 2H), 7.81 (d, $J$ = 8.3 Hz, 1H), 7.11 (d, $J$ = 1.8 Hz, 1H), 7.08 – 7.04 (m, 3H), 6.79 (s, 1H), 6.59 (s, 1H), 4.47 (s, 4H), 4.30 (s, 3H), 4.02 (s, 3H), 3.87 (d, $J$ = 2.5 Hz, 6H). $^{13}$C NMR (101 MHz, $CDCl_3$): δ (ppm) 180.74 (s), 165.74 (s), 163.82 (s), 161.46 (s), 159.57 (s), 158.87 (s), 151.62 (s), 146.72 (s), 139.22 (s), 136.61 (s), 132.97 (s), 132.83 (s), 125.75 (s), 121.29 (s), 119.36 (s), 115.08 (s), 114.84 (s), 111.24 (s), 107.24 (s), 90.54 (s), 68.16 (s), 66.47 (s), 62.40 (s), 61.62 (s), 56.62 (s), 52.09 (s). MS (ESI) m/z: 540.94 $[M + H]^+$, calcd. for $C_{28}H_{25}ClO_9$ 540.12.

*4.1.4.18. 4-Bromo-2-{2-[4-(5,6,7-trimethoxy-4-oxo-4H-chromen-2-yl)-phenoxy]-ethoxy}-benzoic acid methyl ester (compound **7r**)*

Compound **7r** was obtained as yellow solid; yield: 47.0%; m.p: 159.6-162.0 °C; $^1$H NMR (400 MHz, $CDCl_3$): δ (ppm) 7.84 (d, $J$ = 8.1 Hz, 2H), 7.69 (d, $J$ = 8.3 Hz, 1H), 7.24 (s, 1H), 7.18 (d, $J$ = 8.3 Hz, 1H), 7.01 (d, $J$ = 8.1 Hz, 2H), 6.75 (s, 1H), 6.55 (s, 1H), 4.43 (s, 4H), 4.26 (s, 3H), 3.98 (s, 3H), 3.83 (s, 6H). $^{13}$C NMR (101 MHz, $CDCl_3$): δ (ppm) 180.72 (s), 165.83 (s), 163.82 (s), 161.45 (s), 159.56 (s), 158.75 (s), 151.63 (s), 146.72 (s), 136.61 (s), 132.93 (d, $J$ = 6.4 Hz), 127.46 (s), 125.76 (s), 124.30 (s), 119.86 (s), 117.85 (s), 115.08 (s), 111.22 (s), 107.24 (s), 90.54 (s), 68.23 (s), 66.49 (s), 62.41 (s), 61.62 (s), 56.62 (s), 52.11 (s), 29.71 (s). MS (ESI) m/z: 585.10 $[M + H]^+$, calcd. for $C_{28}H_{25}BrO_9$ 584.07.

*4.1.4.19. 2-{4-[4-(5,6,7-Trimethoxy-4-oxo-4H-chromen-2-yl)-phenoxy]-butoxy}-benzoic acid methyl ester (compound **7s**)*

Compound **7s** was obtained as yellow solid; yield: 63.3%; m.p: 120.7-121.3 °C; $^1$H NMR (400 MHz, $CDCl_3$): δ (ppm) 7.91 – 7.80 (m, 3H), 7.54 – 7.44 (m, 1H), 7.03 (dd, $J$ = 14.0, 6.6 Hz, 4H), 6.80 (d, $J$ = 6.6 Hz, 1H), 6.60 (d, $J$ = 6.6 Hz, 1H), 4.33 – 4.27 (m, 3H), 4.17 (s, 4H), 4.03 (d, $J$ = 6.6 Hz,

3H), 3.95 – 3.90 (m, 3H), 3.89 – 3.85 (m, 3H), 2.11 (s, 4H). $^{13}$C NMR (101 MHz, $CDCl_3$): δ (ppm) 180.74 (s), 166.77 (s), 163.79 (s), 161.40 (s), 160.18 (s), 158.48 (s), 151.59 (s), 146.55 (s), 136.58 (s), 133.46 (s), 132.97 (s), 131.68 (s), 125.11 (s), 120.30 (s), 120.20 (s), 114.91 (s), 113.11 (s), 111.56 (s), 107.30 (s), 90.55 (s), 68.30 (s), 67.61 (s), 62.41 (s), 61.63 (s), 56.61 (s), 51.91 (s), 25.92 (s). MS (ESI) m/z: 535.15 $[M + H]^+$, calcd. for $C_{30}H_{30}O_9$ 534.19.

*4.1.4.20. 2-{3-[4-(5,6,7-Trimethoxy-4-oxo-4H-chromen-2-yl)-phenoxy]-propoxy}-benzoic acid methyl ester (compound **7t**)*

Compound **7t** was obtained as yellow solid; yield: 65.4%; m.p: 82.5-84.5 °C; $^1$H NMR (400 MHz, $CDCl_3$): δ (ppm) 7.85 (t, *J* = 7.8 Hz, 3H), 7.50 (t, *J* = 7.9 Hz, 1H), 7.03 (dd, *J* = 8.0, 4.0 Hz, 4H), 6.79 (s, 1H), 6.59 (s, 1H), 4.34 (t, *J* = 5.9 Hz, 2H), 4.29 (d, *J* = 6.8 Hz, 5H), 4.02 (s, 3H), 3.91 (s, 3H), 3.86 (s, 3H), 2.38 (p, *J* = 5.9 Hz, 2H). $^{13}$C NMR (101 MHz, $CDCl_3$): δ (ppm) 180.74 (s), 166.65 (s), 163.79 (s), 161.40 (s), 160.05 (s), 158.36 (s), 151.59 (s), 146.58 (s), 136.58 (s), 133.50 (s), 132.98 (s), 131.70 (s), 125.23 (s), 120.36 (d, *J* = 4.3 Hz), 114.95 (s), 113.25 (s), 111.51 (s), 107.29 (s), 90.55 (s), 65.13 (s), 64.48 (s), 62.41 (s), 61.63 (s), 56.61 (s), 51.92 (s), 29.15 (s). MS (ESI) m/z: 521.08 $[M + H]^+$, calcd. for $C_{29}H_{28}O_9$ 520.17.

*4.1.4.21. 2-{2-[4-(5,6,7-Trimethoxy-4-oxo-4H-chromen-2-yl)-phenoxy]-ethoxy}-benzoic acid methyl ester (compound **7u**)*

Compound **7u** was obtained as yellow solid; yield: 69.5%; m.p: 125.0-127.0 °C; $^1$H NMR (400 MHz, $CDCl_3$): δ (ppm) 7.90 – 7.82 (m, 3H), 7.55 – 7.49 (m, 1H), 7.12 – 7.04 (m, 4H), 6.80 (s, 1H), 6.59 (s, 1H), 4.47 (s, 4H), 4.30 (s, 3H), 4.02 (s, 3H), 3.89 (s, 3H), 3.86 (s, 3H). $^{13}$C NMR (101 MHz, $CDCl_3$): δ (ppm) 180.73 (s), 166.66 (s), 163.81 (s), 161.45 (s), 159.73 (s), 158.14 (s), 151.60 (s), 146.68 (s), 136.60 (s), 133.44 (s), 132.96 (s), 131.66 (s), 125.63 (s), 121.15 (d, *J* = 5.0 Hz), 115.11 (s), 114.42 (s), 111.31 (s), 107.25 (s), 90.56 (s), 67.98 (s), 66.63 (s), 62.40 (s), 61.62 (s), 56.62 (s), 51.99 (s), 29.70 (s).MS (ESI) m/z: 507.13 $[M + H]^+$, calcd. for $C_{28}H_{26}O_9$ 506.16.

*4.1.4.22. 2,3,5-Trichloro-6-{4-[4-(5,6,7-trimethoxy-4-oxo-4H-chromen-2-yl)-phenoxy]-butoxy}-benzoic acid methyl ester (compound **7v**)*

Compound **7v** was obtained as yellow solid; yield: 52.5%; m.p: 70.5-72.7 °C; $^1$H NMR (400 MHz, $CDCl_3$): δ (ppm) 7.87 (d, *J* = 8.8 Hz, 2H), 7.59 (s, 1H), 7.00 (d, *J* = 8.8 Hz, 2H), 6.80 (s, 1H), 6.59 (s, 1H), 4.30 (s, 3H), 4.14 (dt, *J* = 13.9, 5.8 Hz, 4H), 4.02 (s, 3H), 3.99 (s, 3H), 3.86 (s, 3H), 2.10 – 1.96 (m, 4H). $^{13}$C NMR (101 MHz, $CDCl_3$): δ (ppm) 180.74 (s), 164.49 (s), 163.80 (s), 161.41 (s),

160.10 (s), 151.61 (s), 151.45 (s), 146.59 (s), 136.59 (s), 132.98 (s), 131.83 (s), 131.68 (s), 128.85 (s), 128.23 (s), 127.33 (s), 125.23 (s), 114.89 (s), 111.49 (s), 107.29 (s), 90.53 (s), 74.91 (s), 67.52 (s), 62.41 (s), 61.63 (s), 56.61 (s), 53.14 (s), 26.64 (s), 25.71 (s). MS (ESI) m/z: 637.06 $[M + H]^+$, calcd. for $C_{30}H_{27}Cl_3O_9$ 636.07.

*4.1.4.23. 2,3,5-Trichloro-6-{3-[4-(5,6,7-trimethoxy-4-oxo-4H-chromen-2-yl)-phenoxy]-propoxy}-benzoic acid methyl ester (compound **7w**)*

Compound **7w** was obtained as yellow solid; yield: 54.9%; m.p: 60.5-63.0 °C; $^1$H NMR (400 MHz, $CDCl_3$): δ (ppm) 7.89 (s, 2H), 7.62 (d, $J$ = 24.8 Hz, 1H), 7.04 (s, 2H), 6.84 (d, $J$ = 25.3 Hz, 1H), 6.63 (d, $J$ = 25.3 Hz, 1H), 4.34 (d, $J$ = 25.1 Hz, 7H), 4.07 (d, $J$ = 25.1 Hz, 3H), 3.94 (t, $J$ = 23.4 Hz, 6H), 2.31 (s, 2H). $^{13}$C NMR (101 MHz, $CDCl_3$): δ (ppm) 180.73 (s), 164.38 (s), 163.80 (s), 161.43 (s), 159.94 (s), 151.62 (s), 151.21 (s), 146.62 (s), 136.60 (s), 132.99 (s), 131.85 (s), 131.66 (s), 129.02 (s), 128.28 (s), 127.33 (s), 125.35 (s), 114.90 (s), 111.42 (s), 107.28 (s), 90.53 (s), 71.65 (s), 64.08 (s), 62.41 (s), 61.63 (s), 56.61 (s), 53.15 (s), 29.77 (s). MS (ESI) m/z: 622.98 $[M + H]^+$, calcd. for $C_{29}H_{25}Cl_3O_9$ 622.06.

*4.1.4.24. 2,3,5-Trichloro-6-{2-[4-(5,6,7-trimethoxy-4-oxo-4H-chromen-2-yl)-phenoxy]-ethoxy}-benzoic acid methyl ester (compound **7x**)*

Compound **7x** was obtained as yellow solid; yield: 57.0%; m.p: 152.0-154.5 °C; $^1$H NMR (400 MHz, $CDCl_3$): δ (ppm) 7.89 (d, $J$ = 8.6 Hz, 2H), 7.62 (s, 1H), 7.04 (d, $J$ = 8.5 Hz, 2H), 6.80 (s, 1H), 6.59 (s, 1H), 4.51 – 4.46 (m, 2H), 4.39 – 4.35 (m, 2H), 4.30 (s, 3H), 4.03 (s, 3H), 3.96 (s, 3H), 3.87 (s, 3H). $^{13}$C NMR (101 MHz, $CDCl_3$): δ (ppm) 180.74 (s), 164.25 (s), 163.83 (s), 161.47 (s), 159.55 (s), 151.64 (s), 151.00 (s), 146.72 (s), 136.62 (s), 132.97 (s), 131.90 (s), 131.74 (s), 129.35 (s), 128.43 (s), 127.21 (s), 125.73 (s), 115.00 (s), 111.26 (s), 107.25 (s), 90.53 (s), 73.01 (s), 66.67 (s), 62.41 (s), 61.63 (s), 56.62 (s), 53.22 (s), 29.71 (s). MS (ESI) m/z: 609.10 $[M + H]^+$, calcd. for $C_{28}H_{23}Cl_3O_9$ 608.04.

*4.2. Cell culture and incubation procedures*

The human colon cancer cells (HTC116) and the human hepatoma cancer cells (BEL-7402) were obtained from the Type Culture Collection of the Chinese Academy of Sciences, Shanghai, China. The human gastric cancer cells (MGC-803 and HGC-27) were obtained from the National Experimental Cell Resource Sharing Service Platform, Beijing, China. The human gastric cancer cells (SGC-7901) and the human gastric normal epithelial cell line (GES-1) were obtained from the

Advanced Research Center of Central South University, Changsha, China. HCT-116 cells were grown in Dulbecco's Modified Eagle's Medium (DMEM) containing 15% (v/v) fetal bovine serum (FBS), 100 IU/mL penicillin and 100 μg/mL of streptomycin. MGC-803 and GES-1 cells were grown in DMEM containing 10% (v/v) FBS, 100 IU/mL penicillin and 100 μg/mL of streptomycin. BEL-7402, HGC-27 and SGC-7901 cells were grown in Roswell Park Memorial Institute medium (RPMI-1640) containing 10% (v/v) FBS, 100 IU/mL penicillin and 100 μg/mL of streptomycin. All of the cells were maintained in a humidified atmosphere with 5% $CO_2$ at 37 ℃. For the experiments, the cells were removed by trypsinizing (0.025% trypsin, 0.02% EDTA) and washed with phosphate-buffered saline (PBS).

### *4.3. MTT assay for cell proliferation*

Thiazolyl blue tetrazolium bromide (MTT) method was used to evaluate the survival of cells. About $5\times10^3$ cells were placed into each of the 96-well plates and grown for 24 h. Test compounds were dissolved in dimethyl sulfoxide (DMSO) then it was individually added to triplicate the wells at final different concentrations (128, 64, 32, 16, 8, 4, 2, 1 μM). After incubation for 48 h, 20 μL of MTT reagent (5 mg/mL in PBS) were added to each well, the cells were further incubated at 37 °C for 4 h. The supernatant in the well was carefully removed and formazan crystals were dissolved in 150 mL of buffered (DMSO), and shacked for 10 min. The absorbance (optical density, OD) was measured at 490 nm on a Wellscan MK-2 microplate reader. In these experiments, 5-FU was the positive reference and 0.1% DMSO was used as the negative reference. The $IC_{50}$ (concentration needed to inhibit growth of 50%) value was calculated on a GraphPad Prism 6.0 software. All experiments were independently evaluated at least three times.

### *4.4. Colony formation assay*

To evaluate the colony-forming ability of compound **7f**-treated HGC-27 cells, the colony formation assay was conducted. HGC-27 cells were seeded in 6-well plates at a density of 1500 cells/well, then incubated for 24 h. Various concentrations (0, 4, 8 and 16 μM) of compound **7f** were added to the cell culture, and then, the culture medium was replaced with fresh medium and incubated for a definite period time of 9 days at 37 °C. The colonies thus formed were fixed with 4% paraformaldehyde for 15 min, then stained with 0.1% crystal violet for 15 min at RT. After many washes with PBS, the colonies in plates were dried and photographed for studies. Each variant of the experiment was assessed in triplicate and repeated three times.

### *4.5. Wound healing assay*

Wound healing assay was used to investigate the inhibition of compound **7f** on the migration ability of HGC-27 cells. For this experiment, HGC-27 cells were seeded in 6-well plates for 24 h and cultured until 70% confluency was reached. The bottom of the 6-well plate was scratched with a 10 μL sterile pipette tip to create a linear wound in the monolayers of cells. Afterward, the detached cells were removed rinsed with PBS and the culture medium was replaced by fresh medium. Next, compound **7f** was added to the medium at different concentrations (0, 4, 8, 16 μM) and incubated for 48 h. Finally, the photographs were obtained with an inverted-phase microscope.

### *4.6. Hoechst 33258 staining assay*

The nuclear morphological modifications were performed on the fluorescent microscopy using Hoechst staining. In this assay, HGC-27 cells were seeded in 6-well plates with 2 mL of medium. After 24 h of incubation, compound **7f** was added at different concentrations and cells were incubated again for a period of 48 h. After washed twice with PBS, cells were fixed with 4% paraformaldehyde for 15 min and stained with 1 mL of Hoechst 33258 solution for 10 min in the dark at 37 ℃. Finally, they were observed under the fluorescence microscope (Olympus, Japan). All experiments were separately determined in triplicate.

### *4.7. Annexin V-FITC/PI dual staining assay*

Cells apoptosis was analyzed using annexin V-FITC/PI staining by flow cytometry according to the manufacturer's instructions to assess apoptotic cells. The HGC-27 cells were seeded in 6-well plates at a density of $5\times10^5$ cells/well and were incubated with different concentrations of compound **7f** (0, 4, 8 and 16 μM) for 48 h at 37 °C, followed by the addition of 5 μL Annexin V-FITC (fluorescein isothiocyanate) and 5 μL PI (propidium iodide). And then the cells were incubated for 15 min at 25 ℃ in the dark before analysis. Finally, the samples were observed by the FACSCalibur flow cytometry (BD Biosciences, USA) and analyzed on a FlowJo software. All measurements were performed by triplicate.

### *4.8. Cell cycle analysis using flow cytometry*

The cell cycle distribution of HGC-27 cell line treated with compound **7f** was assessed by flow cytometry. HGC-27 cells were seeded in 6-well plates at a density of $2 \times 10^5$ cells and incubated for 24 h (37 °C, 5% $CO_2$). Then, the cells were treated with compound **7f** at several concentrations (0, 4, 8, 16 μM) and incubated for an additional 48 h in triplicate manner. Cells were trypsinized,

harvested, centrifuged (1200 rpm for 10 min) and fixed in ice-cold 70% ethanol at 4 ℃ overnight. And then, cells stained with the propidium iodide (PI) solution (50 μg/ml PI and 200 μg/mL RNAse A) for 30 min under darkness at 37 ℃. Finally, Cell cycle analysis was assessed using FACSCalibur flow cytometry (BD Biosciences, USA). Each experiment was performed in triplicate.

### *4.9. Immunofluorescence staining analysis*

After treatment with compound **7f** at various concentrations (0, 4, 16, and 64 μM) for 48 h, cells grown on 6-well glass slides were fixed with 5% paraformaldehyde (PFA) for 15 min at room temperature, and then blocked with 1% bovine serine albumin (BSA) in PBS for 30 min. Subsequently, cells were incubated with primary antibodies α-Tubulin Rabbit Polyclonal Antibody (1 : 500; Beyotime, CN) at 4 °C overnight., followed by incubation with the secondary antibody Cy3 conjugated Goat Anti-mouse IgG (1 : 250; Servicebio, CN) for 1 h under-protected from light. After staining the nuclei with DAPI (1 : 1000), the confocal dishes were mounted with 90% glycerol in PBS and then examined with a confocal laser microscope (Nikon C2, Japan).

### *4.10. Molecular Docking Simulation*

Molecular docking simulation was executed by the SYBYL-X 2.0. The crystal structure of the tubulin was retrieved from the protein data bank (PDB) (http://www.rcsb.org/, PDB code 1SA0). The synthesized compounds **7f** were sketched in ChemDraw Ultra 7.0. For the docking simulation, the target and ligands were processed using a custom import setting wizard of the docking program. Images depicting the proposed binding modes were produced using PyMOL software.

### *4.11. Lactate measurement*

HGC-27 cells were plated in 6-well plates at a density of 1 $\times 10^5$ cells per well and treated with different concentrations of compound **7f** (0, 4, 8, 16 μM). After 48 h of incubation, the lactic acid (LD) levels in the culture supernatant were determined with the LD determination development kit (Nanjing Jiancheng Bioengineering Institute, Nanjing, China) according to the manufacturer's instructions. The absorbance at 530 nm was measured by a Wellscan MK-2 microplate reader. LD levels were calculated from the following formula:

$$(A-B)/(C-B)*D*E$$

A: The measured absorbance value

B: The blank absorbance value

C: The standard absorbance value

D: The standard concentration

E: The dilution factor before sample test

All experiments were repeated for three times.

### *4.12. Western blot assay*

Western blotting was measured to evaluate the changes in selected protein expression in response to treatment with compound **7f.** In short, HGC-27 cells were incubated with various concentrations (0, 4, 8 and 16 μM) of compound **7f** in triplicate for 48 h under normoxia or hypoxic conditions, respectively. $CoCl_2$ (100 μM) and serum starvation (0.1% FBS) treatment mimicked hypoxic conditions. Then, cells were harvested, lysed in lysis buffer and centrifuged at 15,000 g for 10 min at 4 ℃. After the determination of protein levels, extracted proteins were separated from each other using sodium dodecyl sulfate-polyacrylamide gel electrophoresis (10% gel, SDS-PAGE) and transferred onto a polyvinylidene fluoride (PVDF) membrane. Then, the membranes with selected proteins blocking with 5% non-fat milk in TBST at room temperature for 2 h and incubated at 4 ℃ overnight with the following primary antibodies: HIF-1α (1 : 500; Proteintech, USA), VEGF (1 : 2000; Proteintech, USA), PFKM (1 : 1000; Proteintech, USA), PKM2 (1 : 2000; Proteintech, USA), HK2 (1 : 2000; Proteintech, USA) or β-actin (1 : 5000; Immunoway, USA). The bound antibodies were detected by anti-rabbit horseradish peroxidase-conjugated secondary antibody (1 : 4000; Proteintech, USA) and visualized using an enhanced chemiluminescent reagent (EMD Millipore, Billerica, MA, USA). Gray values of protein bands were quantitatively analyzed, with the gray value of the β-actin band as the reference. Each experiment was performed three times separately.

### *4.13. Statistical Analyses.*

All values were presented as the arithmetic mean value ± SD (standard deviation). Each value is the mean of at least three separate experiments in each group. Statistical analyses were carried out using Origin 8.0 and Prism 6.0 GraphPad software. Student t test was employed for determining comparisons between two groups. One-way ANOVA was used for multiple group comparisons. Statistical significance was set at $P < 0.05$.

## Conflicts of interest

Authors have no conflict of interest to declare.

## Acknowledgments

This work was financially supported by Hunan Provincial Key Laboratory of tumor microenvironment responsive drug research (Approval number: 2019-56) and Hunan Province Cooperative Innovation Center for Molecular Target New Drug Study.

## References

[1] R.J. Deberardinis, J.J. Lum, G. Hatzivassiliou, C.B. Thompson, The biology of cancer: metabolic reprogramming fuels cell growth and proliferation, Cell Metab. 7 (2008) 0-20.

[2] B. Freddie, F. Jacques, S. Isabelle, R.L. Siegel, L.A. Torre, Global cancer statistics 2018: globocan estimates of incidence and mortality worldwide for 36 cancers in 185 countries, Ca-Cancer J. Clin. 68 (2018) 394-424.

[3] C. M. Hartshorn, M.S. Bradbury, G.M. Lanza, A.E. Nel, J. Rao, A.Z. Wang, Nanotechnology strategies to advance outcomes in clinical cancer care, ACS Nano 12 (2018) 24-43.

[4] N. H. Park, W. Cheng, F. Lai, C. Yang, F.D.S. Paola, B. Periaswamy, Addressing drug resistance in cancer with macromolecular chemotherapeutic agents, J. Am. Chem. Soc. 140 (2018) 4244-4252.

[5] N. M. Raghavendra, D. Pingili, S. Kadasi, A. Mettu, P. Svum, Dual or multi-targeting inhibitors: the next generation anticancer agents, Eur. J. Med. Chem. 143 (2018) 1277-1300.

[6] B. Bilanges, N. Torbett, B. Vanhaesebroeck, Killing two kinase families with one stone, Nat. Chem. Biol. 4 (2008) 648-649.

[7] R. Kurzrock, S.I. Sherman, D.W. Ball, A.A. Forastiere, R.B. Cohen, R. Mehra, Activity of xl184 (cabozantinib), an oral tyrosine kinase inhibitor, in patients with medullary thyroid cancer, J. Clin. Oncol. 29 (2011) 2660-2666.

[8] W. Huang, Q. Chen, W.C. Yang, G.F. Yang, Cheminform abstract: efficient synthesis and antiproliferative activity of novel thioether-substituted flavonoids, Cheminform 66 (2013) 161-170.

[9] M. Katalinić, G. Rusak, J.B.G. Domaćinović, D. Sinko, R. Jelić, Antolović, Structural aspects of flavonoids as inhibitors of human butyrylcholinesterase, Eur. J. Med. Chem. 45 (2010) 186-192.

[10] S.F. Fonseca, D.B. Lima, D. Alves, Synthesis, characterization and antioxidant activity of organoselenium and organotellurium compound derivatives of chrysin. New J. Chem. 39 (2015) 3043–3050.

[11] H.D. Shin, H.J. Lee, M.A. Sikder, H.P. Su, J. Ryu, J.H. Hong, Effect of chrysin on gene expression and production of muc5ac mucin from cultured airway epithelial cells, Tub. Res. Dis. 73 (2012) 204-209.

[12] J. Wang, J. Qiu, J. Dong, H. Li, M. Luo, X. Dai, Chrysin protects mice from Staphylococcus aureus pneumonia, J. Appl. Microbiol. 111 (2011) 1551-1558.

[13] E.K. Shin, H.S. Kwon, Y.H. Kim, H.K. Shin, J.K. Kim, Chrysin, a natural flavone, improves murine inflammatory bowel diseases, Biochem. Bioph. Res. Co. 381 (2009) 502-507.

[14] M. Torrespiedra, R. Ortizandrade, R. Villalobosmolina, N. Singh, J. L. Medinafranco, S. P. Webster, A comparative study of flavonoid analogues on streptozotocin-nicotinamide induced diabetic rats: quercetin as a potential antidiabetic agent acting via 11β-hydroxysteroid dehydrogenase type 1 inhibition, Eur. J. Med. Chem. 45 (2010) 2606-2612.

[15] E. Brown, N.S. Hurd, S. Mccall, T.E. Ceremuga, Evaluation of the anxiolytic effects of chrysin, a passiflora incarnata extract, in the laboratory rat, Aana. J. 75 (2007) 333.

[16] K.B. Yin, C.S. Ling, B. Prabha, Apoptotic effects of chrysin in human cancer cell lines, Int. J. Mol. Sci. 11 (2010) 2188-2199.

[17] M.E. Mohamed, R.F. Frye, Effects of herbal supplements on drug glucuronidation. review of clinical, animal, and in vitro studies, Planta Med. 77 (2011) 311-321.

[18] S. Zhan, B. Yan, Y.Y. Wen, X. Yao, X. Ma, G. Sheng, Vitexin attenuates acute doxorubicin cardiotoxicity in rats via the suppression of oxidative stress, inflammation and apoptosis and the activation of foxo3a, Exp. Ther. Med. 12 (2016) 1879.

[19] L. Wei, Y. Zhou, Q. Dai, C. Qiao, L. Zhao, H. Hui, Oroxylin a induces dissociation of hexokinase ii from the mitochondria and inhibits glycolysis by sirt3-mediated deacetylation of cyclophilin d in breast carcinoma, Cell Death Dis. 4 (2013) e601.

[20] X. Deng, R. Liu, J. Li, Z. Li, J. Liu, R. Xiong, Design, synthesis, and preliminary biological evaluation of 30,40,50-trimethoxy flavonoid salicylate derivatives as potential anti-tumor agents, New J. Chem. 43 (2019) 1874.

[21] S. Sravani, T. Ramya, M.B. Deepti, N. Narayana, K.B. Kiran, Design and synthesis of substituted dihydropyrimidinone derivatives as cytotoxic and tubulin polymerization inhibitors, Bioorg. Chem. 93 (2019) 103317.

[22] M. Zhai, W. Long, S. Liu, L. Wang, Y. Peng, J. Wang, Synthesis and biological evaluation of (1-aryl-1 h -pyrazol-4-yl) (3,4,5-trimethoxyphenyl)methanone derivatives as tubulin inhibitors, Eur. J. Med. Chem. 156 (2018) 137-147.

[23] S. Etiennemanneville, From signaling pathways to microtubule dynamics: the key players, Curr. Opin. Cell Biol. 22 (2010) 104-111.

[24] J. Li, Y. Jamin, J.K. Boult, C. Cummings, J.C. Waterton, J. Ulloa, Tumour biomechanical response to the

vascular disrupting agent ZD6126 in vivo assessed by magnetic resonance elastography, Br. J. Cancer 110 (2014) 1727–1732.

[25] L. Liu, R.P. Mason, B. Gimi, Dynamic bioluminescence and fluorescence imaging of the effects of the antivascular agent combretastatin-A4P (CA4P) on brain tumor xenografts, Cancer Lett. 356 (2015) 462–469.

[26] A.M. Gaya, G.J. Rustin, Vascular disrupting agents: a new class of drug in cancer therapy, Clin. Oncol. 17 (2005) 277–290.

[27] P.E. Thorpe, Vascular targeting agents as cancer therapeutics, Clin. Cancer Res. 10 (2004) 415–427.

[28] C. Stengel, S.P. Newman, M.P. Leese, B.V.L. Potter, M.J. Reed, A. Purohit, Class III beta-tubulin expression and in vitro resistance to microtubule targeting agents, Brit. J. Cancer 102 (2010) 316-324.

[29] Q. Wang, K.E. Arnst, Y. Wang, G. Kumar, D. Ma, H. Chen, Structural modification of the 3,4,5-trimethoxyphenyl moiety in the tubulin inhibitor veru-111 leads to improved antiproliferative activities, J. Med. Chem. 61 (2018) 7877−7891.

[30] C. Scarpignato, R.H. Hunt, Nonsteroidal antiinflammatory drug-related injury to the gastrointestinal tract: clinical picture, pathogenesis, and prevention, Gastroenterol. Clin. N. 39 (2010) 433-464.

[31] R. Hosseinzadeh, K. Khorsandi, M. Jahanshiri, Combination photodynamic therapy of human breast cancer using salicylic acid and methylene blue, Spectrochim. Acta A 184 (2017) 198-203.

[32] H.G. Yu, J.A. Huang, Y.N. Yang, H. Huang, H.S. Luo, J.P. Yu, The effects of acetylsalicylic acid on proliferation, apoptosis, and invasion of cyclooxygenase-2 negative colon cancer cells, Eur. J. Med. Chem. 32 (2015) 838-846.

[33] G.A. Spitz, C.M. Furtado, M. Sola-Penna, P. Zancan, Acetylsalicylic acid and salicylic acid decrease tumor cell viability and glucose metabolism modulating 6-phosphofructo-1-kinase structure and activity, Biochem. Pharmacol. 77 (2009) 46-53.

[34] E.R. Kasala, L.N. Bodduluru, R.M. Madana, R. Gogoi, C.C. Barua, Chemopreventive and therapeutic potential of chrysin in cancer: mechanistic perspectives, Toxicol. Lett. 233 (2015) 214-225.

[35] P. Qiu, H. Guan, P. Dong, S. Li, C.T. Ho, M.H. Pan, The p53, bax and p21 dependent inhibition of colon cancer cell growth by 5-hydroxy polymethoxyflavones, Mol. Nutr. Food Res. 55 (2011) 613-622.

[36] J.A. Pietenpol, Cell-cycle dysregulation and anticancer therapy, Trends Pharmacol. Sci. 24 (2003) 139-145.

[37] C.J. Trabbic, J.H. Overmeyer, E.M. Alexander, E.J. Crissman, H.M. Kvale, M.A. Smith, Synthesis and biological evaluation of indolyl-pyridinyl-propenones having either methuosis or microtubule disruption activity, J. Med. Chem. 58 (2015) 2489-2512.

[38] O.N. Okorie, P. Dellinger, Lactate: biomarker and potential therapeutic target, Crit. Care Clin. 27 (2011) 299-326.

[39] C.V. Dang, Links between metabolism and cancer, Gene. Dev. 26 (2012) 877–890.

[40] S.J. Tseng, I.M. Kempson, K.Y. Huang, H.J. Li, Y.C. Fa, Y.C. Ho, Targeting tumor microenvironment by bioreduction-activated nanoparticles for light-triggered virotherapy, ACS Nano 12 (2018) 9894-9902.

[41] U.E. Martinezoutschoorn, M. Peirispagés, R.G. Pestell, F. Sotgia, M.P. Lisanti, Cancer metabolism: a therapeutic perspective, Nat. Rev. Clin. Oncol. 14 (2016) 11.

[42] J. Folkman, What is the evidence that tumors are angiogenesis dependent? J. Natl. Cancer Inst. 82 (1990) 4–6.

[43] R. Wang, S. Zhou, S. Li, Cancer therapeutic agents targeting hypoxia-inducible factor 1, Curr. Opin. Chem. Biol. 18 (2011) 3168-3189.

[44] G.L. Semenza, Development of novel therapeutic strategies that target HIF-1, Expert Opin. Ther. Targets. 10 (2006) 267-280.

[45] N.C. Denko, Hypoxia, HIF1 and glucose metabolism in the solid tumour, Nat. Rev. Cancer 8 (2008) 705-713.

[46] P. Vaupel, The role of hypoxia-induced factors in tumor progression, Oncologist 9 (2004) 10-17.

[47] W.F. ernando, H.P. Rupasinghe, D.W. Hoskin, Regulation of Hypoxia-inducible Factor-1α and Vascular Endothelial Growth Factor Signaling by Plant Flavonoids, Mini. Rev. Med. Chem. 15 (2015) 479-489.

[48] B. Manolescu, E. Oprea, C. Busu, C. Cercasov, Natural compounds and the hypoxia-inducible factor (HIF) signalling pathway, Biochimie. 91 (2009) 1347-1358.

Highlight

1. Novel 5,6,7-trimethoxy flavonoid salicylate derivatives were synthesized and characterized.

2. Compound **7f** exhibited potent anti-tumor activity in vitro.

3. Compound **7f** was effective in reducing the stability of microtubule cytoskeleton.

4. Docking studies mimicked the possible binding mechanisms of compound **7f** to tubulin.

5. **7f** down-regulated lactate production and glycolysis-related proteins expression.

6. Compound **7f** decreased HIF-1α expression under hypoxic conditions.

Graphical abstract

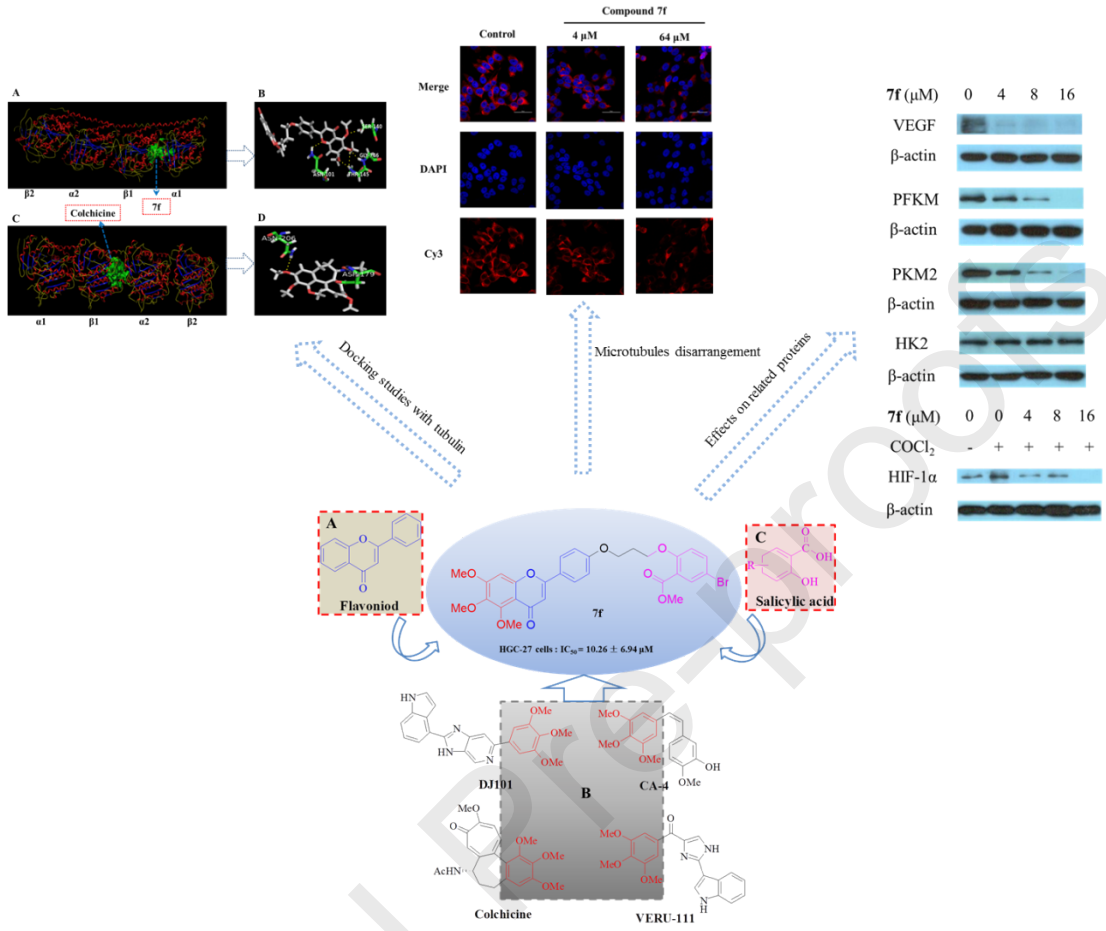

# Conflict of Interest

Authors have no conflict of interest to declare.